Contact size and debris ejection in fretting: The inappropriate use of Archard-type analysis of wear data and the development of alternative wear equations for commonly employed non-conforming specimen pair geometries

T. Zhu[1], P.H. Shipway[1,*]

[1]Faculty of Engineering, University of Nottingham UK

Keywords: wear rate; rate-determining process; cylinder-on-flat; sphere-on-flat; crossed-cylinder

*Corresponding author:

1 Abstract

It has been long understood that fretting differs from sliding wear in that the relative displacement between the bodies is generally smaller than the size of the contact between them, with debris ejection from the contact thus playing an important role in the behaviour of the contact in fretting. Whilst these ideas were clearly articulated more than 30 years ago via Godet's *third-body approach* and Berthier's concept of the *tribology circuit*, calculation of wear rates in fretting have continued to employ Archard's wear equation (or approaches directly derived from it), despite this approach assuming that the rate of wear is controlled by the rate of generation of wear debris (as opposed to the rate of its ejection from the contact).

It has been shown recently that when debris ejection is the rate-determining-process in fretting, the instantaneous rate of wear is inversely proportional to a characteristic dimension of the wear scar. When non-conforming specimen pair geometries (such as cylinder-on-flat) are employed in fretting testing, the wear scar size increases as wear proceeds, and thus the instantaneous rate of wear decreases. In this paper, wear equations have been derived for three commonly employed non-conforming pair specimen geometries, which all take the form $V_w = KR^{n-1}E_d^n$ (V_w is the wear scar volume, R is the radius of the non-plane specimen(s) in the pair and E_d is the frictional energy dissipated) where n varies between 0.67 and 0.8 depending upon the geometry and assumptions made regarding the governing equation. It is argued that the assumptions on which the analysis is based are most valid for the cylinder-on-flat contact configuration with fretting perpendicular to the cylinder axis where the length of the line contact is large compared to the wear scar width.

It is demonstrated that, despite the often apparently good fit of experimental data to an Archard-type equation, it is not appropriate to employ such Archard-type approaches to the analysis of fretting data in situations where debris ejection is the rate-determining-process. The equations derived in this paper relating wear scar size to some measure of the duration of the test should be used for such analysis instead of the linear relationships generally employed in previous work.

2 Introduction

A key aim of much research into wear is the development of an understanding of the relationship between the various parameters which describe the exposure to wear and the amount of wear that results. In the case of fretting wear, the parameters which describe the exposure to wear

include the normal force across the contact, the displacement amplitude, the fretting frequency etc. For applications where the occurrence of fretting wear is common, it is important to understand and quantify how changes in these variables affect the evolution of the wear volume, so that damage can be predicted and its effects on the system controlled.

When analysing bodies of experimental fretting wear data, it is a common practice to aggregate these data into a single parameter to represent and characterise the overall wear behaviour of the whole body. This single parameter is normally identified as the specific *wear rate* and is often presented as the wear volume per unit sliding distance per unit of normal force borne across the contact (after the work of Archard on sliding wear [1]) or the wear volume per unit of frictional energy dissipated proposed by Fouvry and co-workers [2], this itself being derived from the concept espoused by Archard but which also accounts for variations in the coefficient of friction; in this paper, these approaches will be grouped together and termed *Archard-type approaches*. The general agreement on Archard-type approaches has provided common ground for discussion of the effects of individual variables on fretting or for comparisons of the behaviour of different materials to be made across the wide body of literature in this area.

Fretting wear differs from sliding wear in a variety of ways, the most significant being that in fretting, the magnitude of the relative displacement between the bodies is generally much smaller than the size of the contact between those bodies, meaning that debris ejection from the contact needs to be considered as part of the process of continual wear [3, 4]; more specifically, the concept of the "tribology circuit" proposes that in fretting, wear debris elimination from the contact is required for wear to proceed [5]. It is recognised that the rate of debris ejection from the contact will depend upon the size of the contact itself [6] since this "*represents the distance the third body particles must travel* [before ejection from the contact]" [7].

In fretting wear of metals under conditions where debris predominantly consists of metal oxides, there are two key processes, either of which may be the factor that controls the observed rate of wear [8]:

- the rate of formation of the oxide debris (itself dependent amongst other things upon the rate of oxygen ingress into the contact [9-11]);
- the rate of debris ejection from the contact (itself dependent amongst other things upon the contact size and the rheology of the bed [7] and the tendency for the oxide debris particles to agglomerate and potentially sinter [12-14]).

At the start of a test, there will be a transient period where (amongst other things [15]) the debris bed in the contact is building towards a steady state thickness [7]. Once steady state is reached, the rate of debris formation and the rate of its ejection from the contact must be equal [16].

There has been significant recent research progress in considering the effect of transport processes in fretting, both in terms of transport of key species into the contact (in particular oxygen) [11] and in terms of transport of debris out of the contact [8]. Which of these processes is rate-determining will depend upon the conditions under which the fretting is taking place; in particular, it is noted that both transport of key species into the contact and transport of debris out of the contact depend upon the physical size of the wear scar. The work considered in the current paper only addresses situations where debris ejection is rate determining (i.e. it does not address situations where transport of key species into the contact is rate-determining). The recent work by

Baydoun et al. [11] indicates that transport of key species in to the contact will tend to become the rate-determining as the contact size increases and as the time-based rate of wear (i.e. volume lost per unit time) increases.

In concluding that the wear rate may (under certain circumstances) be dependent upon the size of the contact means that under those circumstances, descriptions of wear rate using Archard-type approaches are no longer adequate. Although not explicitly stated, it is implicitly assumed in the Archard-type approaches that the wear rate is governed by the rate of debris formation alone, with this being independent of any transport of species either in or out of the contact. To quote Fillot et al. [16]: "*… Archard's law… primarily focuses on the process of particle detachment. Its goal is only to measure the matter removed from the rubbing surfaces, without taking into account the way this matter protects the materials in contact from further degradation by accommodating the sliding velocity. This is why, when introducing the concept of the third body to understand wear, the latter is redefined as the ejection of the third body outside the contact"*.

The influence of contact size on the rate of fretting may be less of an issue in test programmes where comparisons between different materials or different test conditions are the primary aim of the research, as long as the tests are all conducted with a contact of the same size and with a geometry where the contact size does not change during the course of the test. However, for a variety of reasons, laboratory fretting testing is very often conducted using non-conforming specimen pair configurations where the size of the contact changes as the test proceeds; common geometries of this type are (i) cylinder-on-flat; (ii) sphere-on-flat; (iii) crossed-cylinders. In such configurations, the influence of the radii of the non-plane bodies on the wear rate is well known [9, 17-20]. In such cases, the wear scar increases in size (in a manner dependent upon the geometry of the two first bodies [8]) as wear proceeds [18], and this will result in a change in the rate of debris flow from the contact as the test proceeds. Fillot et al.[16] noted that in the steady state, the rate of formation of debris (i.e. the traditional concept of the "*wear rate*") and the rate of debris flow from the contact must be equal. This idea was developed recently in a paper where the concept of the rate-determining process was outlined [8]; in this, rates of the two processes (debris formation and debris ejection from the contact) are considered separately, with the process with the lower of the two rates at any point in a test being termed *the rate-determining process*. Figure 1 illustrates schematically the two rates as a function of wear scar width, and indicates that for a non-conforming specimen pair configuration (where the wear scar grows as a test proceeds), a change in the rate-determining process may occur during a test as the wear scar grows in size due to continued material removal [8]. It is therefore argued that a nominal measure of the wear scar size (related perhaps to the initial contact size or to the final size [18-20]) is not sufficient in analysis of the evolution of fretting, and that the evolution of the scar size throughout a test needs to be considered and understood.

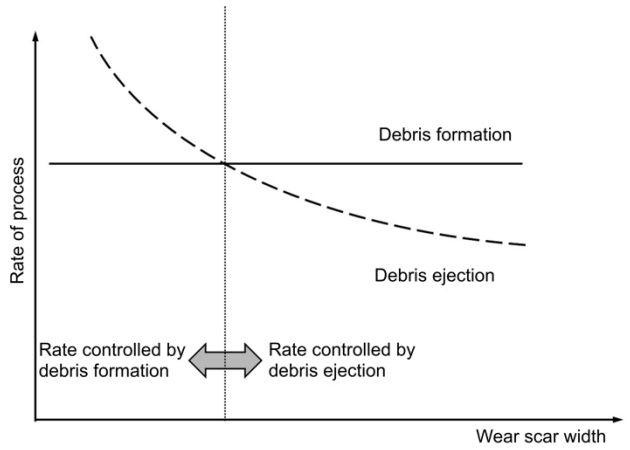

Figure 1: Schematic diagram illustrating the dependence of rates of debris formation and debris ejection on wear scar width, with regions where debris formation and debris ejection are the rate-determining processes (i.e. the process with the lower of the two rates at any scar width) being identified [8].

In the work where the concept of the rate-determining process was proposed [8], the authors demonstrated that for cylinder-on-flat fretting of a high strength steel (with the fretting motion perpendicular to the axis of the cylinder as shown in Figure 2**Error! Reference source not found.**), the instantaneous wear rate was inversely proportional to the wear scar width, x (the scar width being as indicated in Figure 2), indicating that the wear rate was being controlled by debris ejection from the contact for almost the entire duration of each of these tests (i.e. that the period where debris formation was the rate determining process as indicated in Figure 1 could be neglected). This dependence of wear rate on the contact size invalidates the concept of a constant wear rate in configurations with non-conforming pairs in situations where debris ejection is the rate-determining process, and means that Archard-type approaches (with the total amount of wear being proportional to some measure of the exposure to wear) are not appropriate in the analysis of the evolution of wear in such situations.

(a)

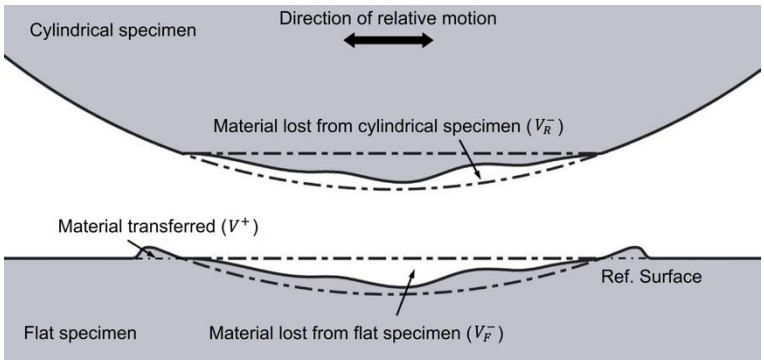

(b)

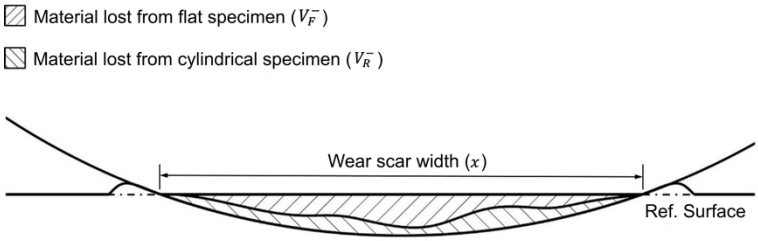

Figure 2: (a) Schematic diagram of distribution of wear across two specimens in a cylinder-on-flat fretting pair (with a small amount of transferred material at the edge), illustrating the assumption (b) that the combined wear on the two specimens result in a total net wear volume equivalent to the minor segment of the cylinder [8].

In that work [8], data were presented relating to the evolution of wear volume (V_w) with frictional energy dissipated (E_d) in fretting for two different geometries of cylinder-on-flat contact, specifically with a cylinder radius, R, of both 6 mm and 160 mm (Figure 3); these were termed $R6$ and $R160$ pairs respectively. As can be seen, the evolution of wear volume with energy dissipated was very different for the two different geometries, and previously, it had been suggested that the Archard-type wear rate was therefore a function of contact geometry [9, 17-20]. However, it was demonstrated in the recent work [8] that these two data sets could be reconciled via the concept of the instantaneous wear rate being proportional to the instantaneous wear scar width; the lines predicting the evolution of wear volume with energy dissipated shown in Figure 3 were both derived from the formulation:

$$\frac{dV_w}{dE_d} = \frac{k_1}{x} \tag{1}$$

where:

$$k_1 = g(P, \delta, T, f \ldots)$$

indicating that the constant k_1 is a function of a number of important parameters in the fretting wear test including the normal load carried by the contact (P), the slip amplitude (δ), the ambient temperature (T), the fretting frequency (f) along with the material properties of the two bodies.

Zhu et al. [8] suggested that the physical rationale behind the form of Equation 1 was based upon either the distance which debris particles need to travel before leaving the contact or upon the concentration gradient down which the debris flow occurs. In the cylinder-on-flat fretting configuration, it was assumed that debris flow was primarily in the direction of the fretting displacement, with this being promoted not only by the action of the displacement itself, but also by the fact that the dimension of the approximately rectangular wear scar parallel to the fretting displacement was small compared to its dimension perpendicular to the fretting direction.

Despite the comments made in the original paper, it is also recognised here that the form of the Equation 1 could also be rationalised in terms of the flow rate of debris out of the contact being inversely proportional to the area of the contact ($A = x\,L$) since L is a constant in a line contact such as this. From this, it might be inferred that the flow rate of debris out of the contact is in fact proportional to the pressure in the contact (namely P/A), although it is also recognised that the

shape of the contact (i.e. the aspect ratio in the case of a rectangular wear scar) is also expected to affect debris flow. The possibility of this being a contact pressure effect is highlighted here since, whilst these two different physical underpinnings are indistinguishable for a line contact, they would lead to different outcomes for an initially point contact (such as sphere-on-flat or crossed-cylinders) which is to be addressed in this work.

A key issue in the previous paper where this concept was first proposed for a cylinder-on-flat fretting contact was that Equation 1 could not be readily transformed into a relationship directly describing the dependence of the wear volume (V_w) upon the energy dissipated (E_d). Instead, both V_w and E_d were described individually as a function of the wear scar width (x) and cylinder radius (R) (amongst other things), yielding a set of parametric equations as follows [8]:

$$V_w = L\left(R^2 \arcsin\left(\frac{x}{2R}\right) - \frac{x}{4}\sqrt{4R^2 - x^2}\right) \tag{2a}$$

$$E_d - E_{th} = m_1 L\left(16R^3 - \sqrt{4R^2 - x^2}(8R^2 + x^2)\right) \tag{2b}$$

where E_{th} is the energy dissipated when wear first begins to occur (often referred to as the threshold energy for onset of wear [21, 22]) and m_1 is a constant related to k_1 from Equation 1, such that $m_1 = \frac{1}{6k_1}$. As such, the way that the wear scar volume evolved with energy dissipated for two very different geometries was rationalised for the first time. Curves were generated from Equation 2 for both $R6$ and $R160$ pairs using the same values of m_1 (i.e. with the same values of k_1) and the same values of E_{th} for the two cases; these curves were plotted against the experimental data and are shown in Figure 3. It can be seen that this approach describes these data well, thus validating the hypotheses that underpin Equation 1.

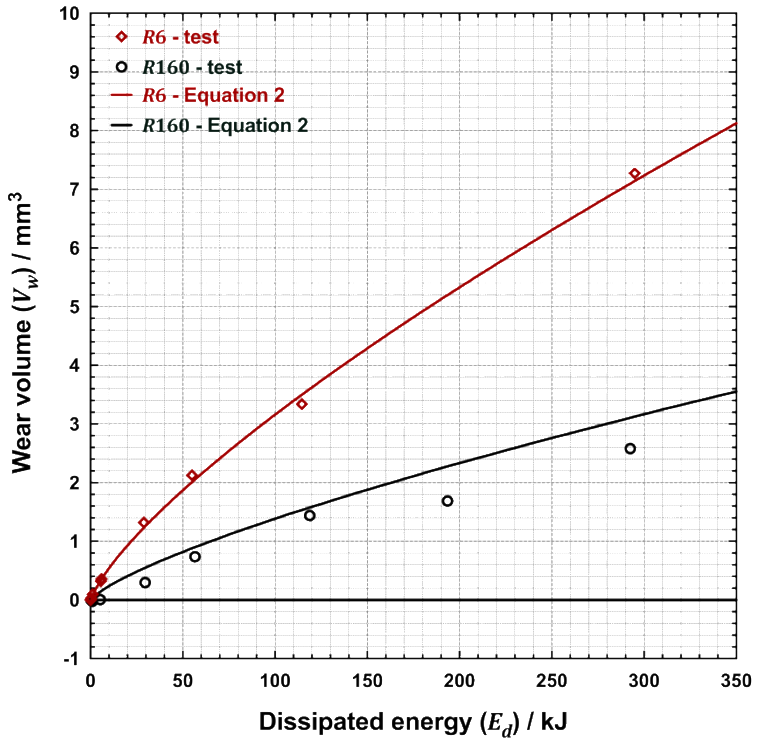

Figure 3: A comparison between the experimental data and the calculated values based on Equation 2 showing the wear volume as a function of dissipated energy for fretting tests conducted with $R6$ pairs and $R160$ pairs [8].

It is noted that the term $(E_d - E_{th})$ represents the frictional energy dissipated above the threshold energy for wear to commence. This will be termed E_{dat} in the current study (the subscript "*dat*" being an acronym for "*dissipated above threshold*") such that $E_{dat} = E_d - E_{th}$.

Despite the success of this formulation in rationalising the data presented in Figure 3, it is recognised that it fails to provide a direct description of the relationship between the wear volume (V_w), the cylinder radius (R) and the energy dissipated (E_d) which is needed to support an understanding of the dependence of the wear volume upon the latter two parameters. Moreover, the formulation of Equation 2 was only derived for a cylinder-on-flat contact and given that other configurations with non-conforming specimen pairs are commonly used in fretting research, there is a need to derive similar equations for those configurations, and in doing so, consider the two plausible forms of the governing equation, namely that the instantaneous wear rate is inversely proportional to a characteristic linear dimension of the scar or that it is proportional to the contact pressure (and thus inversely proportional to the area of the contact). As such, this current work seeks to develop an equation (which we will term the *wear equation*) for situations where a non-conforming specimen pair configuration is employed and where the wear rate is controlled by debris-egress from the contact; for each of the non-conforming specimen pair configurations commonly employed in fretting research (namely cylinder-on-flat, sphere-on-flat and crossed-cylinder geometries), wear equations will be derived which directly describe the relationship between the wear volume (V_w), the energy dissipated (E_d), the relevant geometrical parameters and the initial proposed governing equations.

3 Derivation of a wear equation for a cylinder-on-flat fretting configuration

In the previous study [8], a parametric relationship between wear scar width and wear volume was derived for the cylinder-on-flat configuration (Equation 2) based upon the governing equation (Equation 1) which is valid in describing both of the proposals under consideration, namely (i) that the instantaneous wear rate is inversely proportional to a characteristic linear dimension of the scar or (ii) that the instantaneous wear rate is proportional to the contact pressure (and thus inversely proportional to the area of the contact). To simplify the development of a *wear equation*, the wear scar angle, θ, is now selected as the measure of the progress of wear for a specimen pair (as opposed to the wear scar width, x as was previously selected).

As previously demonstrated [8], the total wear volume across the two samples of a cylinder-on-flat specimen pair is well described by the minor segment of a cylinder defined by the chord of intersection between the cylinder and plane specimens (see Figure 2). The extent of wear is thus described by the angle θ as illustrated in Figure 4, where the wear scar width, x, is equal to $2R\sin(\theta)$.

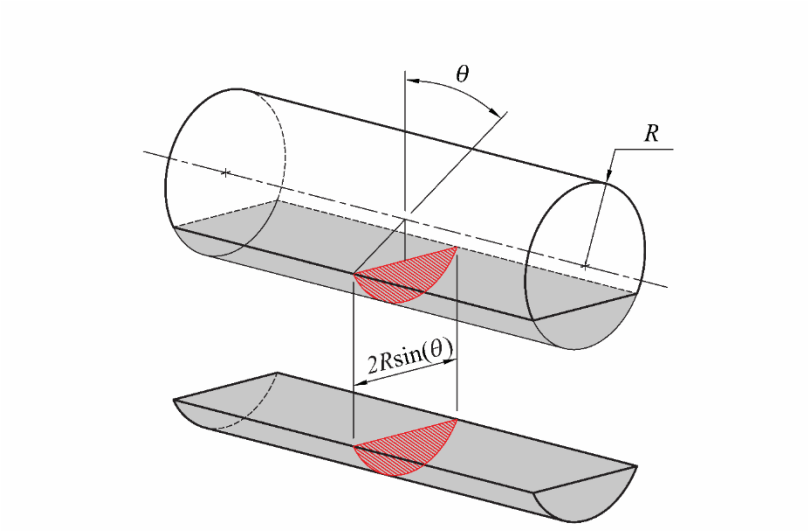

Figure 4: Illustration of the relationship between the wear volume (the minor segment of the cylinder) and its corresponding wear scar angle for the cylinder-on-flat fretting geometry. $0 \leq \theta \leq \frac{\pi}{2}$.

Using the wear scar angle, θ ($0 \leq \theta \leq \frac{\pi}{2}$), allows the parametric equations (Equations 2a and 2b) to be rewritten as follows (see Appendix 4, section A4.1):

$$V_w = LR^2(\theta - \sin(\theta)\cos(\theta)) \tag{3a}$$

$$E_{dat} = m_1 LR^3(\cos(3\theta) - 9\cos(\theta) + 8) \tag{3b}$$

Conducting Taylor series expansions for both Equation 3a and Equation 3b and taking their first non-constant polynomial terms (since these are the dominating terms), approximations for the wear volume and the energy dissipated above the threshold (denoted as $V_w{}'$ and $E_{dat}{}'$ respectively) can be written as follows:

$$V_w{}' = \frac{2}{3} LR^2\theta^3 \tag{4a}$$

$$E_{dat}{}' = 3m_1 LR^3\theta^4 \tag{4b}$$

As can be seen in the next section (Section 3.1), the error associated with the approximations for a cylinder-on-flat contact is relatively low. As such, it is reasonable to assume that $V_w \approx V_w{}'$ when $E_{dat} = E_{dat}{}'$ for all θ, with the approximation being better for smaller values of θ. The formulation of a direct relationship between the wear volume (V_w) and the energy dissipated above the threshold (E_{dat}) is now simply derived by eliminating the wear scar angle, θ, from the approximated equations 4a and 4b, yielding the following relationship:

$$\begin{aligned} V_w &= 2\left(\frac{1}{3}\right)^{1.75}\left(\frac{L}{m_1^3}\right)^{0.25} R^{-0.25} E_{dat}^{0.75} \\ &= A_1 R^{-0.25} E_{dat}^{0.75} \end{aligned} \tag{5}$$

In the previous paper [8], the threshold energy (E_{th}) for the system in question was derived as 560 J, meaning that E_{th} was therefore comparatively small in the context of the maximum values of energy being dissipated in those tests of around 300 kJ (see Figure 3). In situations like this (i.e. tests where the maximum duration is much greater than the duration at which wear is first observed to commence), it seems reasonable therefore to neglect this threshold energy to enable further simplification of the function to take place. This assumption that $E_{th} \approx 0$ allows a further simplification of Equation 5 to yield:

$$V_w = A_1 R^{-0.25} E_d^{0.75} \tag{6}$$

It is recognised that if there is an obvious threshold energy at which wear is first observed in a fretting test dataset, then Equation 5 could readily be employed in preference to Equation 6. However, Equation 6 allows data to be processed where the threshold energy, E_{th}, cannot be readily identified from the dataset available.

3.1 Errors associated with the approximation

The parametric equations given by Equation 3 have been shown to be able to describe well the dependence of wear volume on both energy dissipated and the geometry of the system for the data presented in Figure 3. The approximations of these equations to the forms presented in Equation 4 has then allowed the derivation of the wear equations as presented in Equations 5 and 6. However, the error in moving between the exact equations (Equation 3) to the approximate equations (Equation 4) needs to be understood since the validity (or otherwise) of Equations 5 and 6 are dependent upon this.

Figure 6 shows the relationships between the normalised energy dissipated above the threshold energy ($e_{dat} = \frac{E_{dat}}{m_1 L R^3}$) and the normalised wear volume ($v_w = \frac{V_w}{LR^2}$) for the exact equations (Equation 3) alongside the equivalent for the approximated equations (Equation 4); from the exact form, Equation 3 indicates that the allowable range of e_{dat} is between 0 and 8 and that the allowable range of v_w is between 0 and $\frac{\pi}{2}$ when θ is within the range that $0 \leq \theta \leq \frac{\pi}{2}$. It should be noted that in Figure 5, the axes are normalised to the maximum values, $\max(e_{dat})$ and $\max(v_w)$, respectively ($\max(e_{dat}) = 8$, $\max(v_w) = \frac{\pi}{2}$). It can be seen that the wear volume given by approximated equations is always less than that given by the exact equations for the same value of normalised energy. The error in the wear volume (ε_V) associated with the approximated form when $e_{dat} = e_{dat}'$ is given by:

$$\varepsilon_V = \frac{v_w' - v_w}{v_w} \tag{7}$$

Figure 5 shows that the fractional difference between the normalised wear volume given by the exact and the approximated equations (ε_V) increases as e_{dat} increases, but with the magnitude of the error never being greater than 12%. In the work on which this is based [8], the maximum value of θ observed in the test programme (which included fretting test durations of up to 5×10^6 cycles) was 0.32 which leads to a fractional error, ε_V, of only -0.5%. As such, it can be concluded that the errors in making the approximations of the Taylor series expansions for cylinder-on-flat fretting configurations are small compared to other sources of error, such as in the measurement of

experimental data. As such, we conclude that the wear equation (Equation 6) is a valid equation, with the errors associated with the approximations required for its derivation being of an acceptable magnitude for any amount of wear.

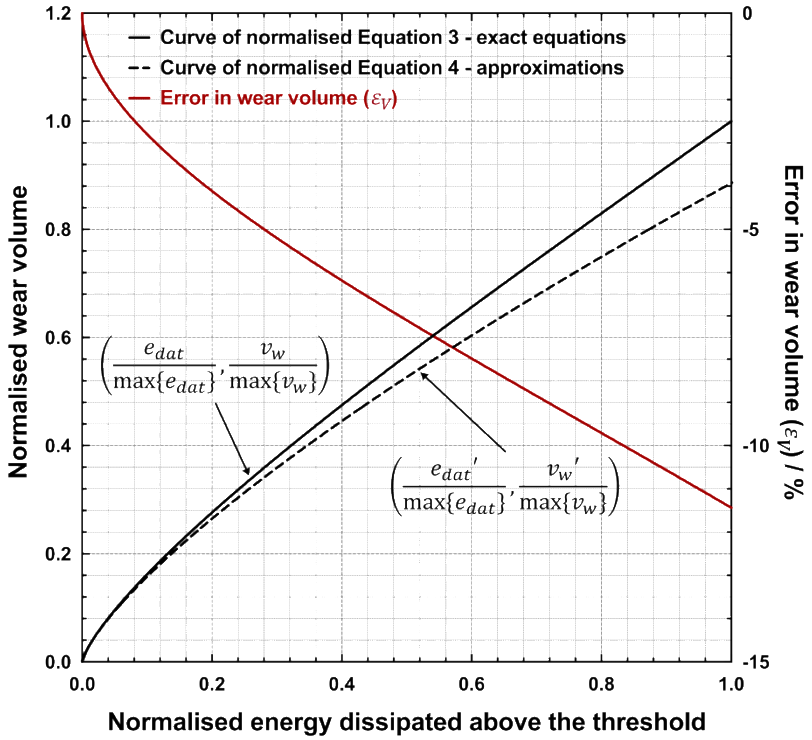

Figure 5: Plot of normalised energy dissipated above the threshold against normalised wear volume for both the exact (Equation 3) and approximate equations (Equation 4) for a cylinder-on-flat contact across the full range of allowable values of e_{dat} along with the fractional error in the wear volume across the same range.

3.2 Experimental verification of the proposed relationship

The wear data from a cylinder-on-flat fretting contact previously presented in Figure 3 are replotted in the form indicated by Equation 6 (i.e. now using the term $R^{-0.25}E_d^{0.75}$ as the abscissa) and presented in Figure 6. Please note that data additional to those presented in Figure 3 are also included in Figure 6; these data relate to tests conducted in exactly the same way as those presented in the previous work [8] but with different cylinder radii in the contact pair, namely 15 mm (data points labelled $R15$) and 80 mm (data points labelled $R80$). It can be seen that the experimental data generated with the four different geometrical configurations are well described across the range of test durations by the function presented in Equation 6. The dashed lines in Figure 6 represent the region of 95% confidence intervals for the overall fitting line.

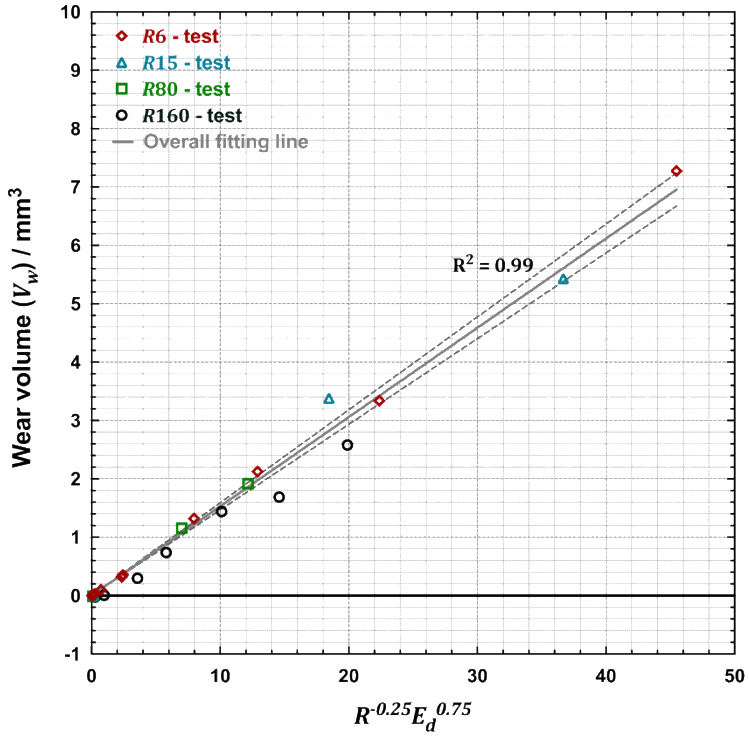

Figure 6: Wear volumes from cylinder-on-flat fretting tests of a high strength steel plotted as a function of $R^{-0.25}E_d^{0.75}$. The data relating to tests with cylinders with radii of 6 mm and 160 mm ($R6$ and $R160$ respectively) are from Figure 3; data related to tests with cylinders with radii of 15 mm and 80 mm ($R15$ and $R80$ respectively) are additional data which relate to experiments with identical materials conducted under the same fretting conditions, but simply with different cylinder radii.

4 Derivation of wear equations for sphere-on-flat and crossed-cylinders fretting configurations

The concept that the instantaneous wear rate may be inversely proportional to a characteristic linear dimension of the scar or that it may be proportional to the contact pressure (and thus inversely proportional to the area of the contact) lead to two different potential governing equations in the case of initially point contacts (i.e. sphere-on-flat and crossed-cylinders geometries). Wear equations based upon the governing equation which states that the instantaneous wear rate is inversely proportional to a characteristic linear dimension of the scar will be derived for the sphere-on-flat and crossed-cylinder contact configurations; however, due to the complexities of the analysis, the wear equation based upon the governing equation which states that the instantaneous wear rate is proportional to the contact pressure (and thus inversely proportional to the area of the contact) will be derived only for the sphere-on-flat contact configuration.

4.1 Wear equations based upon a characteristic linear dimension of the wear scar for the sphere-on-flat and crossed-cylinders contact configurations

The work on the cylinder-on-flat contact configuration presented in Section 3 is simply an extension of the work previously published [8] where Equation 1 was first proposed. In those cylinder-on-flat fretting tests where the fretting motion is perpendicular to the axis of the cylinder and the wear scar dimension perpendicular to the fretting direction is generally much larger than its dimension parallel to the fretting motion, it was assumed that the debris flow velocity out of the

contact was parallel to the direction of the fretting motion; moreover, at any point in the evolution of the wear scar, it was assumed the wear scar width, x, was the same across the length of the contact and could therefore be readily defined.

This geometrical simplicity does not exist in either the sphere-on-flat fretting configuration or the crossed-cylinders fretting configuration. In both cases, the wear scar shape will be equiaxed (assuming that the slip amplitude is small compared to the width of the wear scar); in the case of the sphere-on-flat configuration, the shape of the wear scar projection will be a circle, whereas for the crossed-cylinders geometry, whilst the projection of the wear scar remains equiaxed as wear progresses, it changes shape from circle in the early stages towards a square as wear progresses.

Whilst the fretting displacement will tend to promote debris flow parallel to it, the equiaxed nature of the scars will mean that some (perhaps a significant fraction) of the debris will escape the scar from the sides (termed *side leakage* [23]) which will result in a component of its velocity perpendicular to the fretting direction. As such, there is no intuitively obvious definition of the wear scar width in the direction of the fretting motion over which the debris needs to travel to exit the wear scar.

Despite this complexity, a simple proposal is made at this stage, namely that a characteristic wear scar width can still be defined both for the sphere-on-flat and the crossed-cylinders configurations, with this being the largest value of the scar width parallel to the direction of fretting since it is argued this will be rate-controlling in terms of the debris flow of out of the scar. Using this assumption in each case, and the same methodology as outlined for the cylinder-on-flat contact configuration (as outlined in Section 3), equivalent wear equations can be derived. The details of the methodology for the sphere-on-flat contact configuration are presented in Appendix 1 with those for the crossed-cylinders contact configuration being presented in Appendix 2.

For the sphere-on-flat contact configuration, the wear equation so derived is:

$$V_w = A_2 R^{-0.2} E_d^{0.8} \tag{8}$$

For the crossed-cylinders contact configuration, the wear equation so derived is:

$$V_w = A_3 R^{-0.2} E_d^{0.8} \tag{9}$$

with the basis for the constants A_2 and A_3 as shown in the relevant appendices. It is noted here that the basic form of the wear equations for these two contact types which result in equiaxed wear scar shapes are identical.

4.2 Wear equations based upon a characteristic area of the wear scar for the sphere-on-flat contact configuration

Further to the assumptions made in the derivation of the wear equations in Section 4.1, a second proposal is considered here for the sphere-on-flat contact configuration, namely that that the instantaneous wear rate is inversely proportional to the area of the wear scar. Using this assumption, and the same methodology as outlined for the cylinder-on-flat contact configuration (as outlined in Section 3), an equivalent wear equation can be derived. The details of the methodology are presented in Appendix 3.

For the sphere-on-flat contact configuration, the wear equation so derived is:

$$V_w = A_2 R^{-0.33} E_d^{0.67} \tag{10}$$

4.3 Experimental verification of the proposed relationships for wear scars with equiaxed shapes

Experimental data are available in the literature [19] against which the two wear equations (Equations 8 and Equation 10) for the sphere-on-flat contact configuration can be tested. The data relate to fretting wear of a 52100 steel pair with a sphere-on-flat geometry, with a constant slip amplitude of 72 µm. Three sphere radii were examined, namely 9.525 mm, 25.4 mm and 50 mm; it should be noted that different loads were employed for tests with the three different radii so that the initial Hertzian contact pressure was the same across all three geometries. The wear data are presented in Figure 7 in the form of wear volume as a function of energy dissipated for the three different geometries along with the lines of best fit as proposed in the original paper; it can be seen that the evolution of the wear scar volume with energy is strongly influenced by the geometry of the contacting pairs, with the gradient of the regression lines (previously termed the "*wear rate*") decreasing as the radius of the spherical body was increased. These data are now replotted in the forms indicated by Equation 8 (using the term $R^{-0.2}E_d^{0.8}$ as the abscissa) and by Equation 10 (using the term $R^{-0.33}\ E_d^{0.67}$ as the abscissa) and are presented in Figure 8a and Figure 8b respectively. It can be seen (Figure 8) that the experimental data generated with the different geometrical configurations and test durations are reasonably described by either the function presented in Equation 8 (Figure 8a) or the function presented in Equation 10 (Figure 8b), although it is recognised that the data for the three different sphere radii do still form distinct populations in both cases, indicating that the assumptions made in the derivation of either equation are not entirely valid.

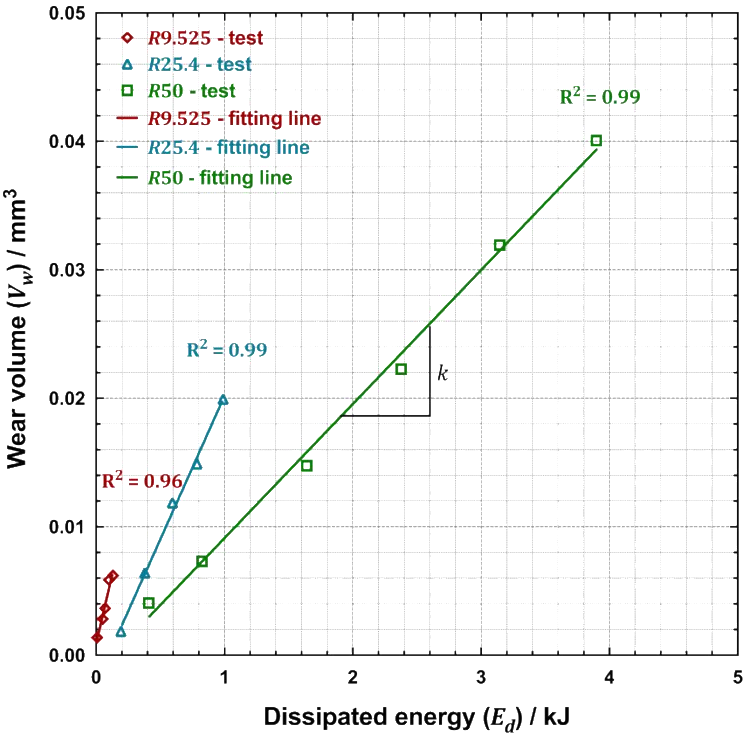

Figure 7: Plot of experimental data from the literature [19] showing the wear volume as a function of dissipated energy for fretting of a high-strength steel conducted with a sphere-on-flat arrangement with three different sphere radii (namely $R9.525$ pairs, $R25.4$ pairs and $R50$ pairs).

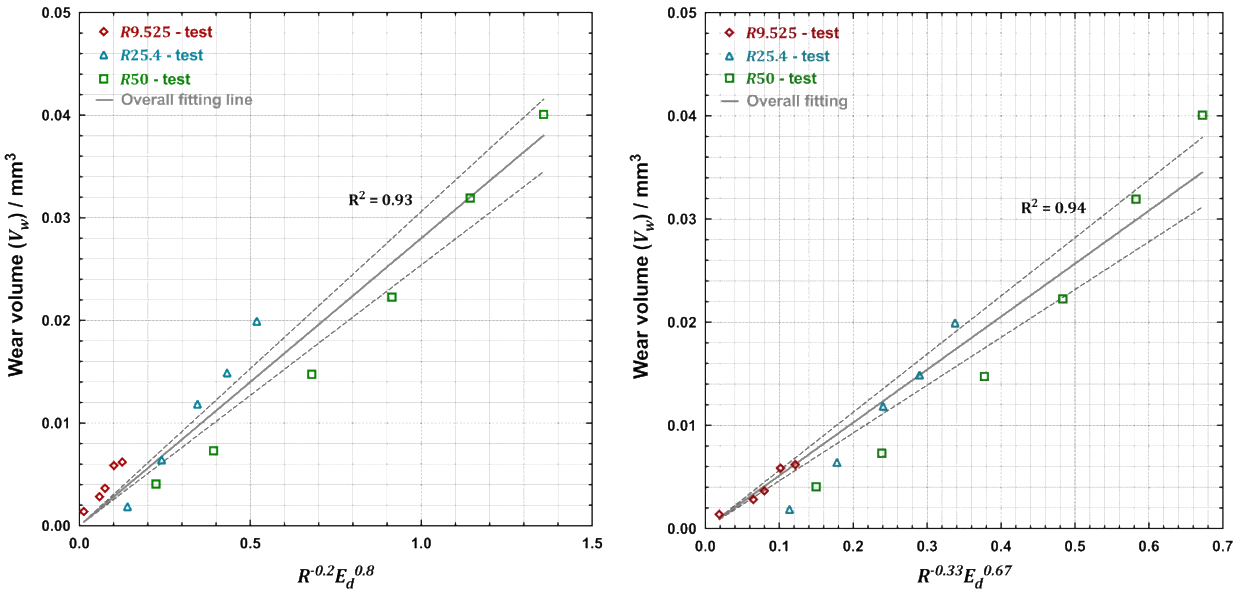

(a) (b)

Figure 8: Replot of data from Figure 7 showing the wear volumes from sphere-on-flat fretting tests of a high strength steel [19] plotted as a function of (a) $R^{-0.2}E_d^{0.8}$; (b) $R^{-0.33}E_d^{0.67}$. The data relate to tests with different sphere radii of 9.525 mm, 25.4 mm and 50 mm.

5 Discussion

5.1 Testing of the wear equations against experimental data

The third body approach [3] and the concept of the tribology circuit [5] both highlight the importance of debris egress from the contact as a critical part of the ongoing process of wear, with the concept of the rate-determining process [8] (either debris formation or debris ejection from the contact) being based upon these. It was shown in this latter work that the rate of debris ejection from the contact was inversely proportional to the wear scar width for a cylinder-on-flat fretting configuration, and parametric equations were derived from which it was demonstrated that the evolution of the wear scar volume with the energy dissipated in the test was non-linear (i.e. Archard-type approaches are not appropriate descriptions of behaviour). However, in that work, the governing formulation was presented in the form of parametric equations which obscured the relationship desired of a wear equation, namely the direct relationship between the wear volume and a measure of the exposure to wear (in this case, the frictional energy dissipated). In the current paper, a wear equation has been derived for the cylinder-on-flat contact which is based upon the same assumptions as employed in the derivation of the parametric equations, namely that the rate of wear is always controlled by debris ejection from the contact (as opposed to debris formation within the contact) and that the threshold energy dissipated (below which there is no wear) is negligible. The wear equation derived is presented in a summary table (Table 1).

The success in providing a coherent framework to understand the differences in development of wear volume in a cylinder-on-flat fretting test as a function of the contact geometry (as can be seen by comparison of Figure 3 and Figure 6) gives support to the underlying assumptions upon which the model development was based, primarily that of wear rate being inversely proportional to the width of the wear scar.

The assumption that the instantaneous wear rate is inversely proportional to the width of the wear scar was employed for the derivation of the equivalent equations for the sphere-on-flat and crossed-cylinders specimen pair configurations (also shown in the summary Table 1). In both of these cases, it is recognised that these begin as a point contacts and that the wear scars remain largely equiaxed as they grow. The assumption is still made in the derivation of the equations that the debris flow out of the contact which occurs in the direction of fretting motion flow controls the wear rate and that the rate is therefore controlled by the largest dimension of the wear scar in that direction; as such, whilst side-leakage of debris from the contact may occur, it is assumed to have no significant influence on the wear rate. Whilst this was a very reasonable assumption for the cylinder-on-flat contact (where the dimension of the wear scar perpendicular to the direction of displacement was large and therefore side-leakage was likely to be a small fraction of the overall debris ejection from the contact), it is clearly less so for these equiaxed contact geometries where side-leakage [3] is a reasonable expectation [5, 24] and may be significant. The equation for development of wear volume for a sphere-on-flat fretting contact based upon the assumption that instantaneous wear rate is inversely proportional to the wear scar radius has been tested against experimental data (Figure 8a) for tests conducted with spheres of different radii. In Figure 8a, the populations associated with the three sphere radii are still distinct (this is in contrast to the equivalent situation for the cylinder-on-flat configuration as presented in Figure 6) and this demonstrates that this wear equation derived is less well able to account for the effect of sphere radius; it is suggested that this indicates that the assumption that side-leakage of debris can be neglected when considering the (rate-determining) rate of debris ejection from the contact is less valid in the sphere-on flat geometry than it is in the cylinder-on-flat geometry. Despite this, the fit of data to the derived form of the wear equation indicated in Figure 8a is still reasonable, indicating the concept of the wear rate being dependent upon the size of the wear scar has clear validity here.

It is noted that the form of Equation 1 used for the broadly rectangular wear scar formed in the cylinder-on-flat contact configuration was also consistent with the assumption that the instantaneous wear rate is inversely proportional to the contact area, a position which would accord with the work in this area which likens the particle bed to a fluid which either flows or is squeezed out of the contact [7, 23]. This second assumption was tested for the case of the sphere-on-flat contact resulting in a wear equation with a slightly different form (Equation 10) which is again included in the summary table (Table 1). Comparison of Figure 8a and Figure 8b indicate that, whilst the data are fully in accord with the concept of the instantaneous wear rate being related to the size of the contact, the area-derived form of the wear equation is no more in accord with the experimental data than the linear-derived form. When the assumptions and the fit to the data for the sphere-on-flat configuration are compared with those for the cylinder-on-flat configuration, it is suggested that the essentially two-dimensional situation of the cylinder-on-flat configuration is preferred: in this case, the debris flow is predominantly parallel to the direction of fretting, driven both by the fretting motion itself and by the fact that the scar dimension in the

fretting direction is small compared to its dimension perpendicular to the fretting motion (with this short distance driving the flow as indicated in the governing equations).

It is noted that no suitable experimental data has been found in the literature against which the form of the wear equation for the crossed-cylinders contact geometry can be tested. However, given the similarity of the developing contact shape between the sphere-on-flat geometry and the crossed-cylinders geometry, it is reasonable to conclude that the wear equation for the latter geometry has similar validity to that of the former geometry.

Table 1: Summary of the wear equations for the three different non-conforming contact configurations considered in this work, namely cylinder-on-flat, sphere-on-flat and crossed-cylinders with both the linear and area bases of the governing equation as indicated.

Contact configurations	Wear equation
Cylinder-on-flat (linear or area)	$V_w = A_1 R^{-0.25} E_d^{0.75}$
Sphere-on-flat (linear)	$V_w = A_2 R^{-0.2} E_d^{0.8}$
Crossed-cylinders (linear)	$V_w = A_3 R^{-0.2} E_d^{0.8}$
Sphere-on-flat (area)	$V_w = A_2' R^{-0.33} E_d^{0.67}$

5.2 Dependence of wear on contact geometry and energy dissipated

The equations for the different contact geometries and assumptions regarding the governing equation are presented in summary in Table 1. In all four cases, the equations take the form (when threshold energy is assumed to be negligible compared to the total dissipated energy into the contact):

$$V_w = K R^{n-1} E_d^n \tag{11}$$

It is noted that K will have units which depend upon the pair geometry and assumptions regarding the governing equation; also, it is noted that (in contrast to the units of the constant in Archard-type formulations), K will not have units which have a clearly recognisable physical meaning and this fact will make the approach being proposed intrinsically less attractive than the traditional approach to the those engaged in research and development in this area.

It was the apparent differences in the fretting wear rates observed as a function the radius of the non-plane members when using both cylinder-on-flat and sphere-on-flat geometries [9, 17-20] that prompted the research in this area (both in a prior paper [8] and in the work reported herein), with its focus on the effect of the developing contact size on the rate of wear. The equations presented in Table 1 allow the dependence of the development of wear volume on the details of the selected test specimen pair geometry to be accounted for; we see that for all three geometrical configurations examined and with the assumptions of both the linear and area dependencies of the instantaneous wear rate, the radius exponent $n-1$ is within the range of $-0.33 \leq n-1 \leq -0.2$, which indicates that for a given energy dissipated, the wear volume will decrease with increasing radius of the non-plane specimen in each case. This is a direct result of the fact that as the specimen radius increases, the scar size will be larger for a given worn volume, with that larger wear scar size then reducing the flow rate of the debris from the contact (Equation 1, Equation

A1.1, Equation A2.1 and Equation A3.1) and thus reducing the rate of wear. However, it is recognised that the dependence on the specimen geometry is relatively weak; for example, for the cylinder-on-flat contact geometry, a change in the cylinder radius by a factor of ~ 27 (as in the experiments reported in Figure 3 and Figure 6) is predicted to result in a change in the wear volume (all other things being equal) by a factor of only ~ 2.3. Notwithstanding, for the first time, these equations have provided a means of incorporating characteristics of the specimen test geometry into the wear equation with the success of this approach being demonstrated most strongly for the cylinder-on-flat test configuration (Figure 6) but also for the sphere-on-flat test configuration (Figure 8) to a lesser extent (the difference being associated with the effects of side-leakage of debris as previously discussed).

Perhaps more significant is the proposed dependence of the wear volume on the energy dissipated. Archard's wear equation [1] was derived for sliding wear, and describes the rate of debris generation in a sliding contact. It has been argued previously (an argument which is reinforced here) that simply applying this equation (or those of other Archard-type approaches) to fretting contacts where debris elimination from the contact is the rate-determining process is not appropriate [16]. The equations (Table 1) derived in this work do (for the first time) take account of the size of the wear scars for the three contact geometries considered with two hypotheses regarding the governing equations, but also give an indication as to why Archard-type equations have been employed so widely in analysis of fretting data. The dependence of wear volume on dissipated energy takes the form as indicated in Equation 11, where across the three geometries examined and with the assumptions of both the linear and area dependencies of the instantaneous wear rate, $0.67 \leq n \leq 0.8$. The fact that these exponents are not far removed from unity (this being the exponent associated with the Archard-type equations) means that the fitting of experimental data to an equation of the form $V_w = kE_d + c$ (where k is considered to be the wear rate and c is a constant representing an initial transient in wear associated with bedding-in [25]) is often apparently quite successful. It is noted that c is often set to zero, with this being a necessary assumption in the many cases reported in the literature where the wear rate k is derived from tests conducted with a single value of energy dissipated, E_d.

To illustrate this, a dataset was formed of 1001 equally-spaced points in E_d and values of wear volume calculated for each of those points according to the relationship $V_w = KE_d^{0.75}$ (i.e. the form relevant to a cylinder-on-flat contact configuration). Linear regressions of the form $V_w = kE_d$ and $V_w = kE_d + c$ were then applied to this dataset. The regression lines to these data are shown in Figure 9a, where the solid line represents the data of the form $V_w = KE_d^{0.75}$ and the dashed lines represent the two different forms of linear regression to these data; it can be seen that it is apparently not unreasonable to apply a linear relationship of either of these types to such a dataset (in both cases, the coefficient of determination, $\mathrm{R}^2 > 0.99$). Moreover, with the natural errors associated with experimental data, the apparent appropriateness of a linear fit to a set of experimental data of this form is even more understandable.

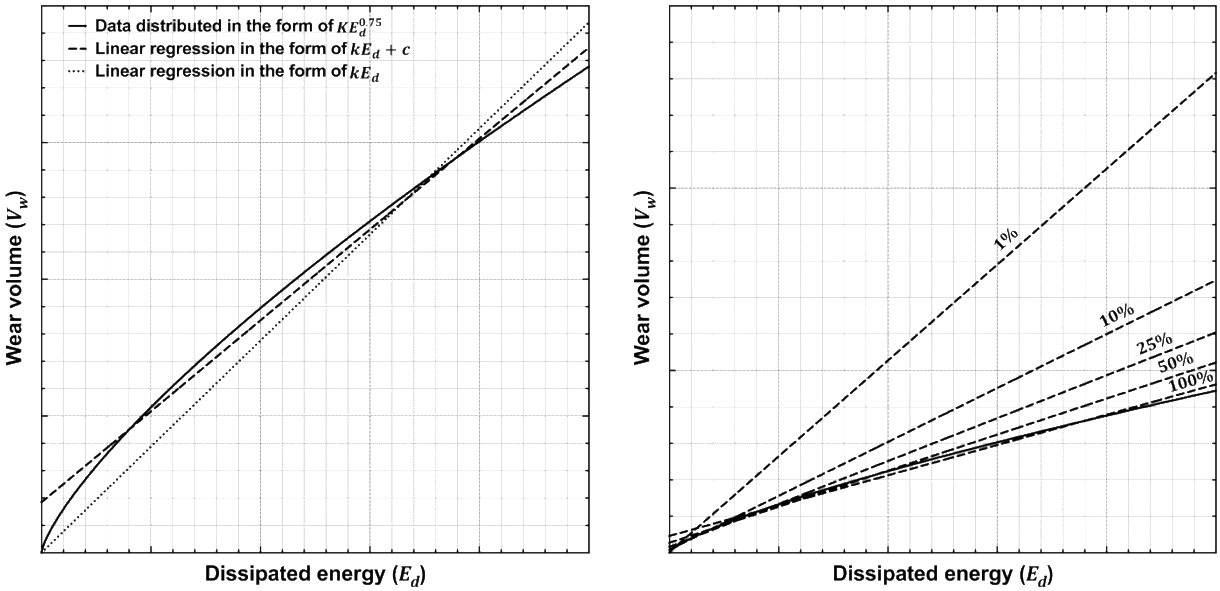

(a) (b)

Figure 9: Schematic diagram showing data distributed in the form $V_w = K E_d^{0.75}$ (solid line) along with linear regressions to those data; (a) linear fit in the form $V_w = k E_d$ (long dashes) and $V_w = k E_d + c$ (short dashes); (b) linear regression in the form $V_w = k E_d + c$ to data from tests of five different durations; the test with the longest duration (in terms of E_d is labelled 100%) with the four shorter tests having a maximum dissipated energy of 1%, 10%, 25% and 50% of that of the longest test. The linear regressions to the datasets from the tests with the five different durations are as indicated by the dashed lines.

If it is (incorrectly) assumed is that the relationship between wear volume (V_w) and energy dissipated (E_d) (or any similar measure of the exposure to wear) is in fact linear (of the general form $V_w = kE_d + c$), then given that enough data have been gathered to identify the value of the initial transient (c) and to ensure that steady-state conditions have been established, the duration of the test (in terms of the total energy dissipated) should not affect the value of the wear rate derived.(It is noted that in previous work, it is not clear that the tests lengths were always adequately long, especially for more conforming contact geometries, to allow steady state conditions to be established as can be seen by a comparison of the data in references [9] and [8]). However, if it is instead assumed (as is argued here) that the data actually take the form $V_w = KE_d^{0.75}$, the gradient of any linear regressions to such data will depend upon the duration of the test (i.e. the maximum value of E_d in the dataset). This is schematically illustrated in Figure 9b; here five tests are simulated with the only difference between those tests being their duration (in terms of E_d). The four shorter tests have durations of 1%, 10%, 25% and 50% of that of the longest test. Linear regressions (of the type $V_w = kE_d + c$) are applied over the data from the five test durations (labelled 100% for the test with the longest duration and then 1%, 10%, 25% and 50% for those of the shorter durations). It is notable again that in each of these cases, the coefficient of determination, $\mathrm{R}^2 > 0.99$. It can be thus seen that the k (traditionally assumed to be the wear rate) is strongly dependent upon the duration of the test, with this gradient decreasing as the duration of the test, E_d, is increased. To give some measure of the significance of these changes, the variation in k with the test duration (represented by E_d) is presented in Figure 10. The implication of this is that when employing a non-conforming geometry for a fretting test programme, if two otherwise identical tests are conducted with different test durations, then the

gradient, k (of the general form $V_w = kE_d + c$) of the linear regression to the resulting data is dependent upon the ratio of the test durations. For example, whichever form (either $V_w = kE_d + c$ or $V_w = kE_d$) is assumed, increasing the test duration by a factor of 10 leads to a reduction of k (the Archard-type wear rate) to 56% of its former value. In fact, the linear regression line is close to the tangent line of data distribution; the gradient of the linear regression can be approximated as the derivative of Equation 11, i.e. it can be shown that as $E_d \to \alpha E_d$, $\frac{dV_w}{dE_d}(\alpha E_d) = \alpha^{n-1}\frac{dV_w}{dE_d}(E_d)$ (with n being defined as in Equation 11) and thus the change of k (the Archard-type wear rate) follows a similar pattern.

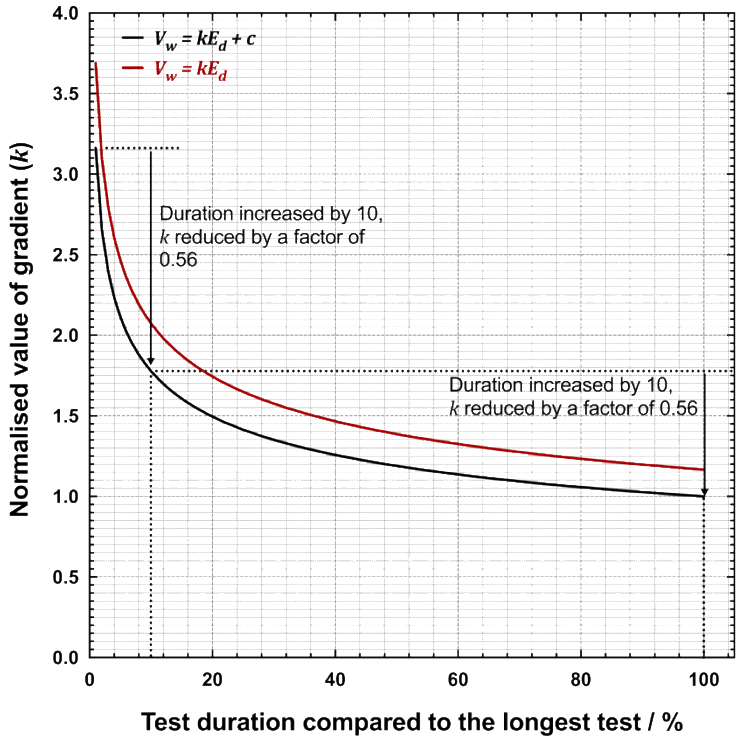

Figure 10: Normalised values of the gradients (k) of linear regressions to data of the form $V_w = KE_d^{0.75}$ with for data of a range of durations, E_d, compared to that of the duration of the longest dataset. Linear regressions both of the form $V_w = kE_d$ and $V_w = kE_d + c$ are shown. The values of k have been normalised to that resulting from the regression of the form $V_w = kE_d + c$ to the longest dataset.

To further illustrate this, linear regression (to the general form $V_w = kE_d + c$) was applied to the experimental data presented in Figure 3 for the 6 mm radius cylinders for different maximum test durations; in each case all the data available both at and below the defined test duration were employed for the linear regression. The gradient of the linear regression (k) to the experimental data is plotted against the test duration as shown in Figure 11; it can be seen that k falls as the test duration was increased, but that in all cases, the coefficient of determination remained high, giving (false) confidence that the experimental data were well described by the form of the equation $V_w = kE_d + c$. The ratio of dissipated energy between the test with the largest and smallest duration here is ~ 50. The ratio α^{n-1} indicates that the gradient of the linear regression (k) should be 2.65 times larger at the smallest duration than at the largest, with the data in Figure 11 demonstrating an equivalent ratio of 2.26. The accord between observations and predictions here adds further weight to this approach.

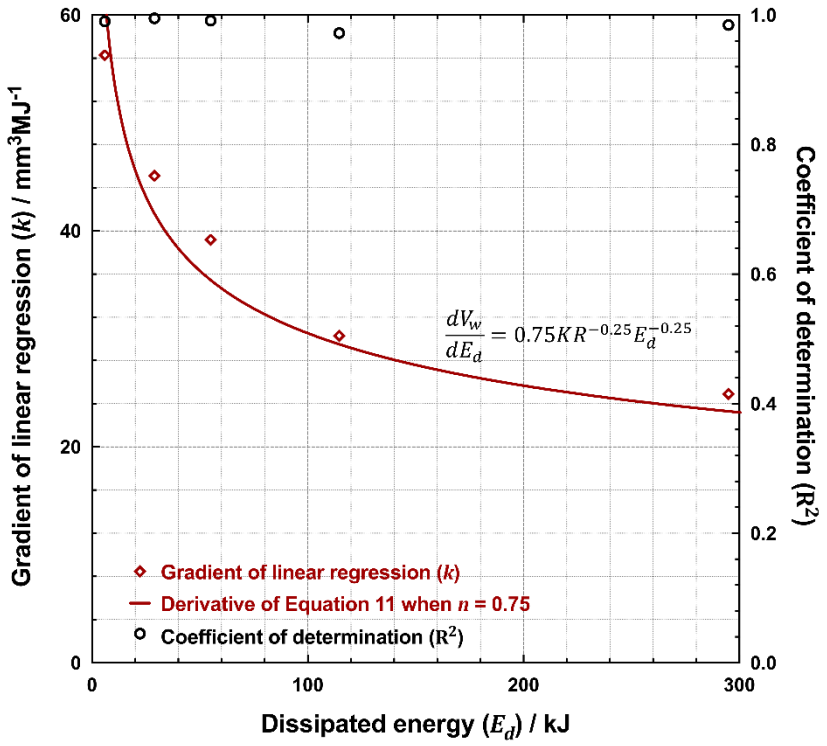

Figure 11: Plot of gradients, k, (of the form $V_w = kE_d + c$) along with the associated coefficients of determination from linear regression of the data for the 6 mm radius cylinders presented in Figure 3 as a function of the maximum energy included in the linear regression.

As such, we see that for fretting conditions where debris ejection from the contact is the rate determining process, linear regression to the general form $V_w = kE_d + c$ generally produces a good fit to the data, but that the high quality of the fit unfortunately provides misplaced assurance that the gradient of such a regression can be regarded as the wear rate. The true form of the relationship $(V_w = KR^{n-1}E_d^n)$ indicates the dependence upon both the geometrical make-up of the contact (R) and the duration of the test (E_d) since both of these affect the development of the size of the contact. It is recognised that K itself is likely to be a function of many other parameters which are regarded as variable in the fretting test such as applied load, slip amplitude, environmental temperature, fretting frequency etc. However, this constant K is independent of test durations and contact geometry and will facilitate understanding of the development of wear in fretting, both in service and in laboratory testing. Whilst these equations have been derived for specific test geometries, the need to consider debris ejection from the contact as a potential rate-determining process is general to all situations where fretting occurs; moreover, it is argued that in any situation where debris egress is seen to be rate-determining (irrespective of geometry), the instantaneous wear rate will be inversely proportional to a characteristic dimension of the size of the wear scar related either to the distance over which debris have to migrate before they can be ejected or to the area of the contact. For laboratory tests where a non-conforming specimen pair geometry is employed, it is recognised that it is helpful to have data across a wide range of values of dissipated

energy, or to have data with the specimen pairs having non-plane specimens over a range of radii, and to plot those data via the appropriate form of wear equation $V_w = KR^{n-1}E_d^n$.

6 Conclusions

It has been shown that under certain circumstances, the *instantaneous wear rate* in fretting is either inversely proportional to a characteristic dimension of the wear scar (the maximum size of the scar parallel to the direction of fretting) or is inversely proportional to the wear scar area. This means that when non-conforming specimen pair geometries are employed in fretting testing (where the scar size grows as wear proceeds), then the instantaneous wear rate changes as the test proceeds. On outcome of this assertion is that the traditional concept of wear rate for such a test is meaningless since it is constantly changing.

Wear equations have been generated for three commonly employed non-conforming specimen pair geometries with the assumptions of both the linear and area dependencies of the instantaneous wear rate which describe the evolution of wear volume with test duration (which is here described by the frictional energy dissipated). The basis of these equations is that of debris-flow out of the contact, and it is shown that the simple assumption that the debris flow rate is inversely proportional to the maximum size of the scar parallel to the direction of fretting is most reasonable when that dimension of the scar is small compared to the size of the scar in other directions. As such, the validity of the equations developed is much higher for cylinder-on-flat test configurations than it is for sphere-on-flat or crossed-cylinders test configurations.

Examination of the form of the wear equations developed provides an understanding of how Archard-type approaches have been inappropriately employed for so long in fretting research, despite the wide consensus regarding the validity of Godet's third body approach and Berthier's tribology circuit which indicate the key role of debris egress from the contact; moreover, it also provides an indication as to how the test duration will affect the traditional measure of the wear rate derived from inappropriate application of an Archard-type equation to such data.

Competing interests: We have no competing interests.

Funding statement: TZ is a PhD student at the University of Nottingham and his work and studentship are funded by the University of Nottingham.

Acknowledgements: The authors thank the University of Nottingham for both financial and facility support. The authors also thank Mr Matthew G. Shipway for his comments and insights during the preparation of this manuscript.

7 References

1. Archard, J.F., *Contact and rubbing of flat surfaces.* Journal of Applied Physics, 1953. **24**(8): p. 981-988.
2. Fouvry, S., P. Kapsa, H. Zahouani, and L. Vincent, *Wear analysis in fretting of hard coatings throught a dissipated energy concept.* Wear, 1997. **203-204**: p. 393-403.
3. Godet, M., *The third-body approach: a mechanical view of wear.* Wear, 1984. **100**(1 - 3): p. 437 - 452.
4. Hurricks, P.L., *The mechanism of fretting - a review.* Wear, 1970. **15**(6): p. 389 - 409.
5. Berthier, Y., *Experimental evidence for friction and wear modeling.* Wear, 1990. **139**(1): p. 77 - 92.
6. Godet, M., D. Play, and D. Berthe, *An attempt to provide a unified treatment of tribology through load carrying capacity, transport and continuum mechanics.* Journal of Tribology, 1980. **102**(2): p. 153-164.
7. Fillot, N., Y. Berthier, and I. Iordanoff, *Simulation of wear through mass balance in a dry contact.* Journal of Tribology, 2005. **127** (1): p. 230-237.
8. Zhu, T., P.H. Shipway, and W. Sun, *The dependence of wear rate on wear scar size in fretting; the role of debris (third body) expulsion from the contact.* Wear, 2019. **440**(203081).
9. Warmuth, A.R., P.H. Shipway, and W. Sun, *Fretting wear mapping: The influence of contact geometry and frequency on debris formation and ejection for a steel-on-steel pair.* Proceedings of the Royal Society A: Mathematical, Physical and Engineering Science, 2015. **471**(2178).
10. Baydoun, S. and S. Fouvry, *An experimental investigation of adhesive wear extension in fretting interface: Application of the contact oxygenation concept.* Tribology International, 2020. **147**: p. art. no. 106266.
11. Baydoun, S., P. Arnaud, and S. Fouvry, *Modelling adhesive wear extension in fretting interfaces: An advection-dispersion-reaction contact oxygenation approach.* Tribology International, 2020. **151**: p. art. no. 106490.
12. Pearson, S.R., P.H. Shipway, J.O. Abere, and R.A.A. Hewitt, *The effect of temperature on wear and friction of a high strength steel in fretting.* Wear, 2013. **303**(1-2): p. 622-631.
13. Hayes, E.K. and P.H. Shipway, *Effect of test conditions on the temperature at which a protective debris bed is formed in fretting of a high strength steel.* Wear, 2017. **376 - 377**(Part B): p. 1460 - 1466.
14. Kirk, A.M., P.H. Shipway, W. Sun, and C.J. Bennett, *Debris development in fretting contacts: debris particles and debris beds.* Tribology International, 2019. **149**: p. art. no. 105592.
15. Liu, Y., T. Liskiewicz, and B. Beake, *Dynamic changes of mechanical properties induced by friction in the Archard wear model.* Wear, 2019. **428-429**: p. 366-375.
16. Fillot, N., I. Iordanoff, and Y. Berthier, *Wear modeling and the third body concept.* Wear, 2007. **262**(7 - 8): p. 949 - 957.
17. Warmuth, A.R., S.R. Pearson, P.H. Shipway, and W. Sun, *The effect of contact geometry on fretting wear rates and mechanism for a high strength steel.* Wear, 2013. **301**(1 - 2): p. 491 - 500.
18. Fouvry, S., C. Poulins, and S. Deyber, *Impact of contact size and complex gross–partial slip conditions on Ti–6Al–4V/ Ti–6Al–4V fretting wear.* Tribology International, 2009. **42**(3): p. 460 - 473.
19. Fouvry, S. and R. Merhej, *Introduction of a power law formulation to quantify the contact size effects on friction and wear responses of dry oscillating sliding contacts: Application to a chromium steel interface.* Wear, 2013. **301**: p. 34-46.
20. Fouvry, S., P. Arnaud, A. Mignot, and P. Neubauer, *Contact size, frequency and cyclic normal force effects on Ti–6Al–4V fretting wear processes: An approach combining friction power and contact oxygenation.* Tribology International, 2017. **113**(September 2017): p. 460-473.
21. Sauger, E., S. Fouvry, L. Ponsonnet, P. Kapsa, J.M. Martin, and L. Vincent, *Tribologically transformed structure in fretting.* Wear, 2000. **245**(1-2): p. 39-52.

22. Pearson, S.R. and P.H. Shipway, *Is the wear coefficient dependent upon slip amplitude in fretting? Vingsbo and Söderberg revisited.* Wear, 2015. **330 - 331**(May - June 2015): p. 93 - 102.
23. Iordanoff, I., Y. Berthier, S. Descartes, and H. Heshmat, *A review of recent approaches for modeling solid third bodies.* Journal of Tribology, 2002. **124**(4): p. 725-735.
24. Colombie, C., Y. Berthier, A. Floquet, L. Vincent, and M. Godet, *Fretting: Load carrying capacity of wear debris.* Journal of Tribology, 1984. **106**(April): p. 194-201.
25. Blau, P.J., *How common is the steady-state? The implications of wear transitions for materials selction and design.* Wear, 2015. **332-333**(May-June): p. 1120-1128.
26. Gradshteyn, I.S. and I.M. Ryzhik, *Table of Integrals, Series, and Products (Seventh Edition)*. 7 ed. 2007, USA: Academic Press. 408.
27. Artin, E., *The Gamma Function*. Dover edition ed. 2015: Dover Publications, Inc.

Appendix 1: Derivation of an equation to describe the relationship between wear volume and energy dissipated for sphere-on-flat contacts assuming wear scar width dependence of wear rate

As for the cylinder-on-flat contact, it is proposed that the instantaneous wear rate is inversely proportional to a characteristic wear scar width (i.e. the wear scar diameter, $2r$) as follows:

$$\frac{dV_w}{dE_d} = \frac{k_2}{2r} \qquad (A1.1)$$

where:

$$k_2 = g(P, \delta, T, f \ldots)$$

indicating that the constant k_2 is a function of various test parameters as previously defined.

As for the cylinder-on-flat case, it is assumed that the total wear volume across the two components of a sphere-on-flat specimen pair can be described by the spherical cap of intersection of the sphere with the plane. The extent of wear is again defined by the wear scar angle θ as illustrated in Figure 12, where the diameter of the circular wear scar, $2r$, is equal to $2R\sin(\theta)$.

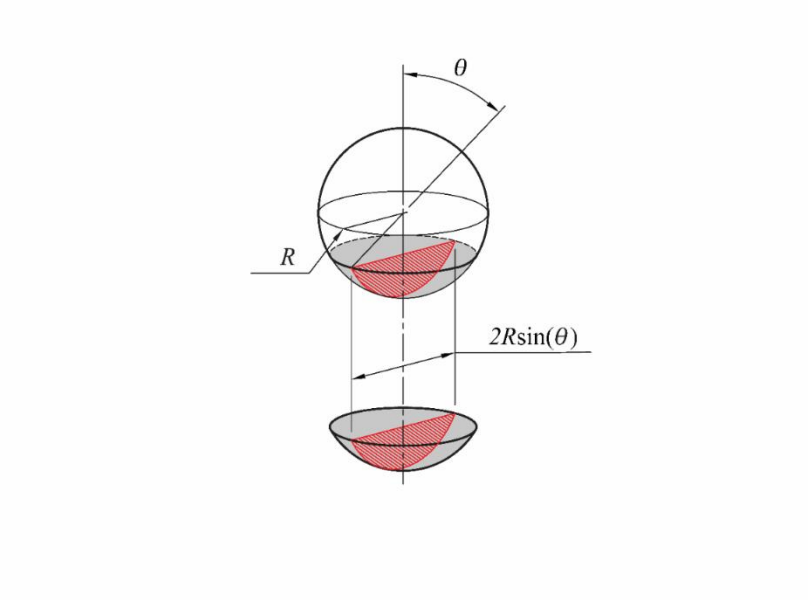

Figure 12: Illustration of the relationship between the wear volume (defined by a spherical cap) and its corresponding wear scar angle for the sphere-on-flat fretting geometry. $0 \leq \theta \leq \frac{\pi}{2}$.

Parametric equations for both the wear volume and the energy dissipated above the threshold energy as functions of the wear scar angle θ can be derived as follows (see Appendix 4, section A4.2):

$$V_w = \frac{\pi R^3}{12}(\cos(3\theta) - 9\cos(\theta) + 8) \qquad (A1.2a)$$

$$E_{dat} = m_2 \pi R^4 (\sin(4\theta) - 8\sin(2\theta) + 12\theta) \qquad (A1.2b)$$

By performing Taylor series expansions for both Equations A1.2a and A1.2b and again taking their first non-constant polynomial terms, the wear volume and the energy dissipated above the threshold can be approximated (denoted as $V_w{}'$ and $E_{dat}{}'$ respectively) as follows:

$$V_w{}' = \frac{\pi R^3 \theta^4}{4} \qquad (A1.3a)$$

$$E_{dat}{}' = \frac{32}{5} m_2 \pi R^4 \theta^5 \qquad (A1.3b)$$

Again, as shown in the next section concerning error analysis for the sphere-on-flat contact (Section A1.1), the error associated with the approximation is relatively low, which leads to the conclusion that $V_w \approx V_w{}'$ when $E_{dat} = E_{dat}{}'$ for all θ, with the approximation being better for smaller values of θ. The formulation of a direct relationship between the wear volume (V_w) and the energy dissipated above the threshold (E_{dat}) is now simply derived by eliminating the wear scar angle, θ, from the approximated equations presented in Equations A1.3a and A1.3b, yielding the following relationship:

$$\begin{aligned} V_w &= \frac{1}{4}\left(\frac{5}{32}\right)^{0.8}\left(\frac{\pi}{m_2^4}\right)^{0.2} R^{-0.2} E_{dat}^{0.8} \\ &= A_2 R^{-0.2} E_{dat}^{0.8} \end{aligned} \qquad (A1.4)$$

As for the cylinder-on-flat configuration, using the assumption that $E_{th} \approx 0$ here allows a further simplification of Equation A1.4 to yield a simplified wear equation for a sphere-on-flat contact in fretting:

$$V_w = A_2 R^{-0.2} E_d^{0.8} \qquad (A1.5)$$

A1.1 Errors associated with the approximation

As for the cylinder-on-flat case, the approximate parametric equations have allowed a wear equation (Equation A1.4) to be derived. However, as before, the errors associated with moving from the exact parametric equations (Equation A1.2) to the approximated parametric equations (Equation A1.3) need to be understood in order that the validity of the approximation can be assessed.

The method by which the errors associated with the approximation are as described in Section 3.1 of the main body of the paper and will not be described again in detail, with simply the outputs being presented. Figure 13 shows the relationship between the normalised energy dissipated above the threshold energy ($e_{dat} = \frac{E_{dat}}{m_2 \pi R^4}$) and the normalised wear volume ($v_w = \frac{V_w}{\pi R^3}$) across the full range of allowable wear scar angles θ ($0 \leq \theta \leq \frac{\pi}{2}$) for the exact equations (Equation A1.2). Alongside is plotted the equivalent relationship for the approximated equations (Equation A1.3) across the same range. It should be noted that in Figure 13, the axes are normalised to the maximum values, $\max(e_{dat})$ and $\max(v_w)$ respectively

($\max(e_{dat}) = 6\pi$, $\max(v_w) = \frac{2}{3}$). It can be seen from Figure 13 that across the full range of allowable wear scar angles, the magnitude of the error in the wear volume associated with the approximations (ε_V, defined in Equation 7) is never greater than 11%. As such, we conclude that wear equation (Equation A1.5) (which has been derived from the Taylor series expansions and the additional assumption that $E_{th} \approx 0$) is a valid equation, with the errors associated with the approximations required for its derivation being of an acceptable magnitude for any amount of wear.

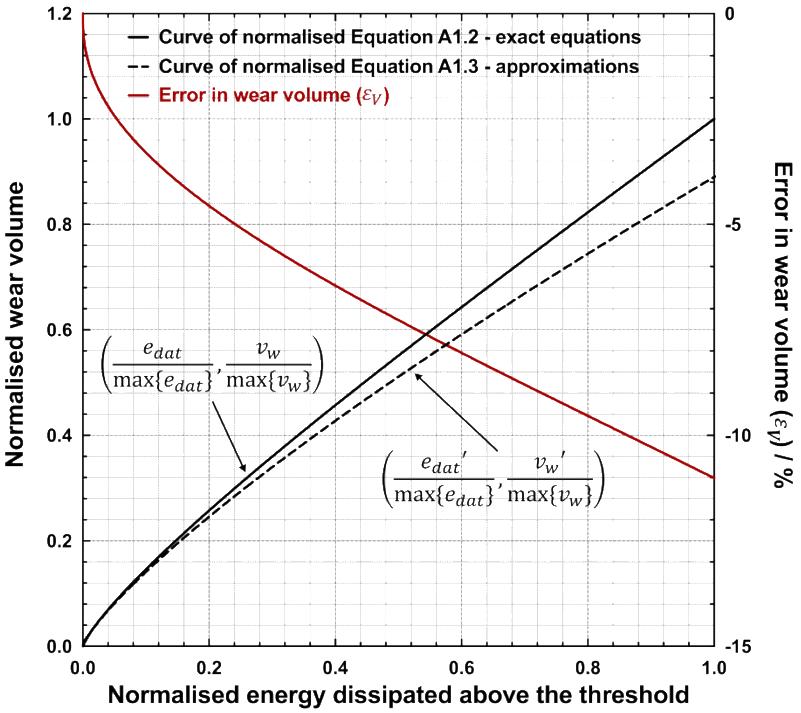

Figure 13: Plot of normalised energy dissipated above the threshold against normalised wear volume for both the exact (Equation A1.2) and approximate equations (Equation A1.3) for a sphere-on-flat contact across the full range of allowable values of e_{dat} along with the fractional error in the wear volume across the same range.

Appendix 2: Derivation of an equation to describe the relationship between wear volume and energy dissipated for a crossed-cylinder contact assuming wear scar width dependence of wear rate

Here, it is proposed that the instantaneous wear rate is again inversely proportional to the characteristic wear scar width, i.e. the maximum scar width parallel to the direction of fretting (w):

$$\frac{dV_w}{dE_d} = \frac{k_3}{w} \qquad (A2.1)$$

where:

$$k_3 = g(P, \delta, T, f \ldots)$$

indicating that the constant k_3 is a function of various parameters as previously defined.

As was previously assumed for the other two geometrical configurations, it is again assumed that the total wear volume across the two components of a crossed-cylinders specimen pair can be described by the volume of intersection of two crossed cylinders. The extent of wear is again defined by the wear scar angle θ as illustrated in Figure 14, where the maximum of wear scar width, w, is equal to $2R\sin(\theta)$.

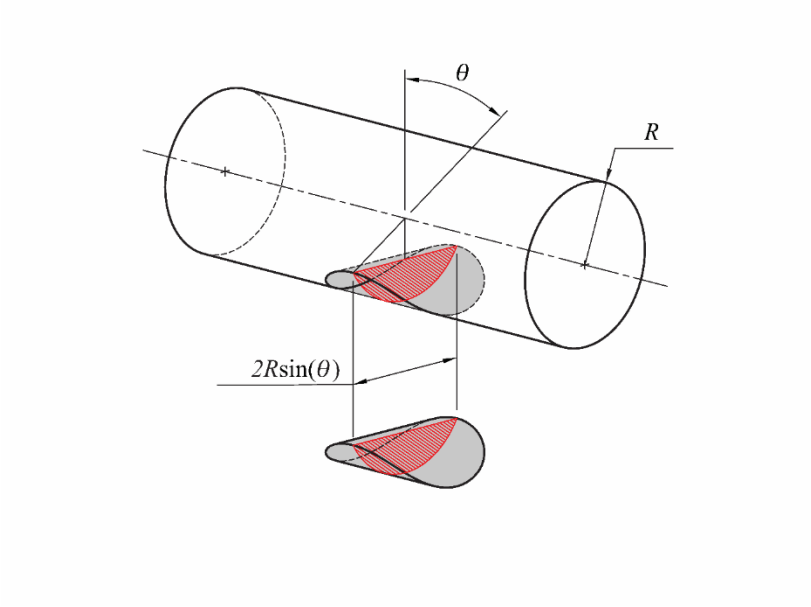

Figure 14: Illustration of the relationship between the wear volume (intersection of two crossed cylinders) and its corresponding wear scar angle for the crossed-cylinders fretting geometry. $0 \leq \theta \leq \frac{\pi}{2}$.

Parametric equations for both the wear volume and the energy dissipated above the threshold energy as functions of the wear scar angle θ can be derived as follows (see Appendix 4, section A4.3):

$$V_w = \frac{\pi R^3}{16}(\cos(3\theta) + 2\cos(2\theta) - 17\cos(\theta) + 14) \qquad (A2.2a)$$

$$E_{dat} = m_3\pi R^4(9\sin(4\theta) + 16\sin(3\theta) - 120\sin(2\theta) - 48\sin(\theta) + 204\,\theta) \qquad (A2.2b)$$

By performing Taylor series expansions for both Equation A2.2a and Equation A2.2b and taking only their first non-constant polynomial terms, the wear volume and the energy dissipated above the threshold can be approximated (denoted as $V_w{}'$ and $E_{dat}{}'$) as follows:

$$V_w{}' = \frac{\pi R^3\theta^4}{4} \qquad (A2.3a)$$

$$E_{dat}{}' = \frac{384}{5} m_3\pi R^4\theta^5 \qquad (A2.3b)$$

Again, as shown in the next section concerning error analysis for the crossed-cylinders contact (Section A2.1), the error associated with the approximation is relatively low, which leads to the conclusion that $V_w \approx V_w{}'$ when $E_{dat} = E_{dat}{}'$ for all θ, with the approximation being better for smaller values of θ. The formulation of a direct relationship between the wear volume (V_w) and the energy dissipated above the threshold (E_{dat}) is now simply derived by eliminating the wear scar angle, θ, from the approximated equations presented in Equations A2.3a and A2.3b, yielding the following relationship:

$$\begin{aligned} V_w &= \frac{1}{4}\left(\frac{5}{384}\right)^{0.8}\left(\frac{\pi}{m_3^4}\right)^{0.2} R^{-0.2}E_{dat}^{0.8} \\ &= A_3 R^{-0.2}E_{dat}^{0.8} \end{aligned} \qquad (A2.4)$$

Using the aforementioned assumption that $E_{th} \approx 0$ allows a further simplification of Equation A2.4 to yield:

$$V_w = A_3 R^{-0.2}E_d^{0.8} \qquad (A2.5)$$

A2.1 Errors associated with the approximation

As before, the errors associated with moving from the exact parametric equations (Equation A2.2) to the approximated parametric equations (Equation A2.3) need to be understood in order that the validity of the approximation can be assessed.

The method by which the errors associated with the approximation are as descried in Section 3.1 of the main body of the paper and will not be described again in detail, with simply the outputs being presented. Figure 15 shows the relationships between the normalised energy dissipated above the threshold energy ($e_{dat} = \frac{E_{dat}}{m_3\pi R^4}$) and the normalised wear volume ($v_w = \frac{V_w}{\pi R^3}$) across the full range of allowable wear scar angles θ ($0 \le \theta \le \frac{\pi}{2}$) for the exact equations (Equation A2.2). Alongside is plotted the equivalent relationship for the approximated equations (Equation A2.3) across the same range. It should be noted that in Figure 15, the axes are normalised to the maximum values, $\max(e_{dat})$ and $\max(v_w)$ respectively ($\max(e_{dat}) = 102\pi - 64$, $\max(v_w) = \frac{3}{4}$). It can be seen from Figure 15 that across the full range of allowable wear scar angles, the magnitude of the error is never greater than 13%. As such, we conclude that the wear equation (Equation A2.5) (which has been derived from the Taylor

series expansions and the additional assumption that $E_{th} \approx 0$) is a valid equation, with the errors associated with the approximations required for its derivation being of an acceptable magnitude for any amount of wear.

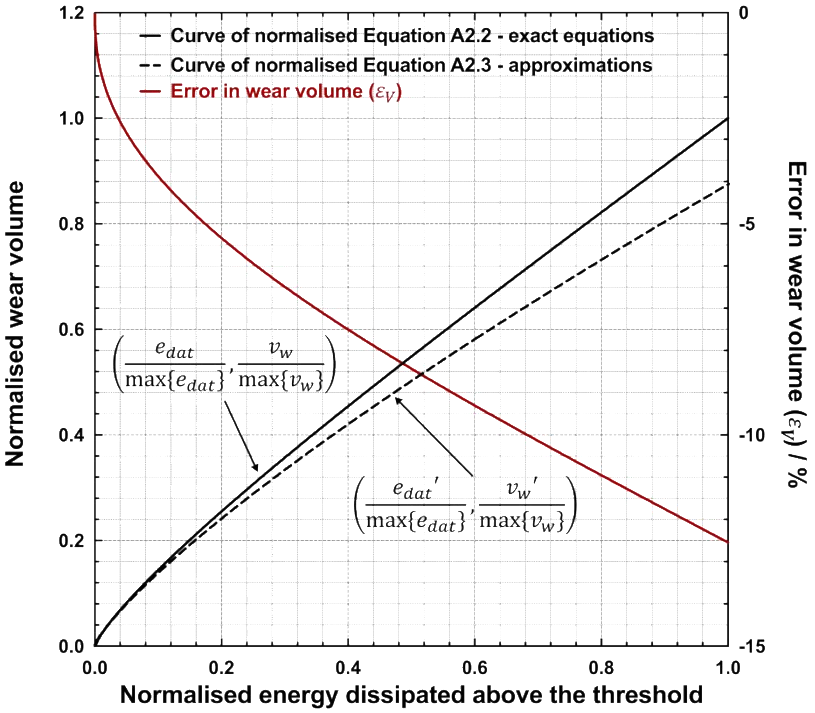

Figure 15: Plot of normalised energy dissipated above the threshold against normalised wear volume for both the exact (Equation A2.2) and approximate equations (Equation A2.3) for a crossed-cylinders contact across the full range of allowable values of e_{dat} along with the fractional error in the wear volume across the same range.

Appendix 3: Derivation of an equation to describe the relationship between wear volume and energy dissipated for a sphere-on-flat contact assuming wear scar area dependence of wear rate

Here, it is proposed that the instantaneous wear rate is inversely proportional to the circular wear scar area, A, as follows (the characteristic wear scar width in Appendix 1, $2r$, is defined as the diameter of the area):

$$\frac{dV_w}{dE_d} = \frac{k_2'}{A} \qquad (A3.1)$$

where:

$$k_2' = g(P, \delta, T, f \ldots)$$

indicating that the constant k_2' is a function of various test parameters as previously defined.

Similar to the definition in Appendix 1, the extent of wear is again defined by the wear scar angle θ as illustrated in Figure 12, where the diameter of the circular wear scar, $2r$, is equal to $2R\sin(\theta)$. Therefore, the area of wear scar for the sphere-on-flat contact, A, can be calculated as $R^2 \sin^2(\theta)$.

Parametric equations for both the wear volume and the energy dissipated above the threshold energy as functions of the wear scar angle θ can be derived as follows (see Appendix 4, section A4.3):

$$V_w = \frac{\pi R^3}{12}(\cos(3\theta) - 9\cos(\theta) + 8) \qquad (A3.2a)$$

$$E_{dat} = m_2'\pi^2 R^5(-3\cos(5\theta) + 25\cos(3\theta) - 150\cos(\theta) + 128) \qquad (A3.2b)$$

By performing Taylor series expansions for both Equations A3.2a and A3.2b and again taking their first non-constant polynomial terms, the wear volume and the energy dissipated above the threshold can be approximated (denoted as $V_w{}'$ and $E_{dat}{}'$ respectively) as follows:

$$V_w{}' = \frac{\pi R^3 \theta^4}{4} \qquad (A3.3a)$$

$$E_{dat}{}' = 40 m_2'\pi^2 R^5 \theta^6 \qquad (A3.3b)$$

Again, as shown in the next section concerning error analysis for the sphere-on-flat contact (Section A3.1), the error associated with the approximation is relatively low, which leads to the conclusion that $V_w \approx V_w{}'$ when $E_{dat} = E_{dat}{}'$ for all θ, with the approximation being better for smaller values of θ. The formulation of a direct relationship between the wear volume (V_w) and the energy dissipated above the threshold (E_{dat}) is now simply derived by eliminating the wear scar angle, θ, from the approximated equations presented in Equations A3.3a and A3.3b, yielding the following relationship:

$$V_w = \frac{1}{4}\left(\frac{1}{40}\right)^{0.67}\left(\frac{1}{\pi {m_2'}^2}\right)^{0.33} R^{-0.33} E_{dat}^{0.67}$$
$$= A_2' R^{-0.33} E_{dat}^{0.67} \quad (A3.4)$$

As for the cylinder-on-flat configuration, using the assumption that $E_{th} \approx 0$ here allows a further simplification of Equation A3.4 to yield a simplified wear equation for a sphere-on-flat contact in fretting:

$$V_w = A_2' R^{-0.33} E_d^{0.67} \quad (A3.5)$$

A3.1 Errors associated with the approximation

The method by which the errors associated with the approximation are as described in Section 3.1 of the main body of the paper, with simply the outputs being presented. Figure 16 shows the relationship between the normalised energy dissipated above the threshold energy ($e_{dat} = \frac{E_{dat}}{m_2' \pi^2 R^5}$) and the normalised wear volume ($v_w = \frac{V_w}{\pi R^3}$) across the full range of allowable wear scar angles θ ($0 \leq \theta \leq \frac{\pi}{2}$) for the exact equations (Equation A3.2). Alongside is plotted the equivalent relationship for the approximated equations (Equation A3.3) across the same range. In Figure 16, the axes are normalised to the maximum values, $\max(e_{dat})$ and $\max(v_w)$ respectively ($\max(e_{dat}) = 128$, $\max(v_w) = \frac{2}{3}$). It can be seen from Figure 16 that across the full range of allowable wear scar angles, the magnitude of the error in the wear volume associated with the approximations (ε_V, defined in Equation 7) is never greater than 19%. As such, we conclude that wear equation (Equation A3.5) (which has been derived from the Taylor series expansions and the additional assumption that $E_{th} \approx 0$) is a valid equation, with the errors associated with the approximations required for its derivation being of an acceptable magnitude for any amount of wear.

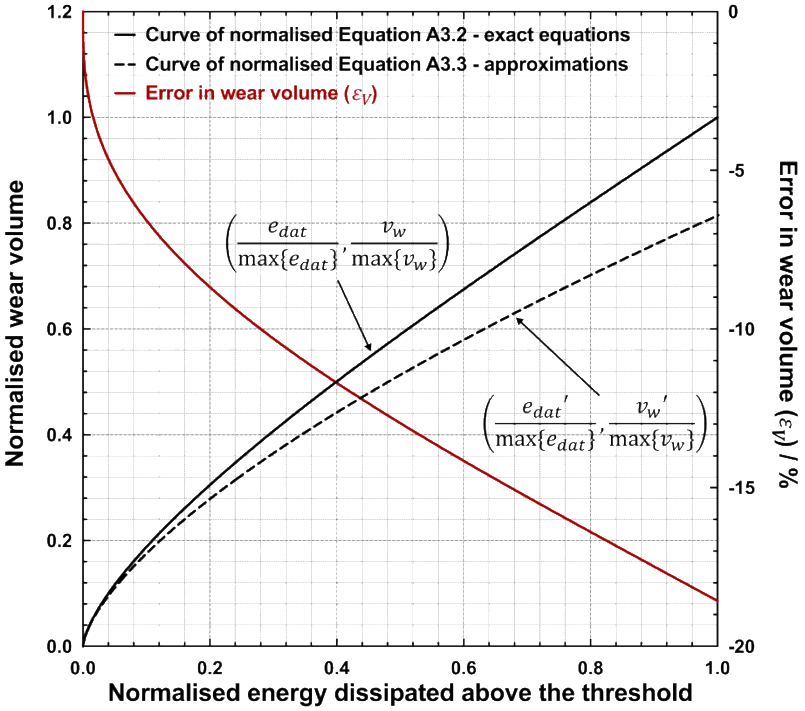

Figure 16: Plot of normalised energy dissipated above the threshold against normalised wear volume for both the exact (Equation A3.2) and approximate equations (Equation A3.3) for a sphere-on-flat contact across the full range of allowable values of e_{dat} along with the fractional error in the wear volume across the same range.

Appendix 4: Details of the methodology for the derivation of the wear equations for all three contact configurations

The steps to determine the relationship between wear volume (V_w) and dissipated energy (E_d) for all three configurations (cylinder-on-flat, sphere-on-flat and crossed-cylinders) are identical, and can be categorised as follows:

(i) derive an expression for V_w in terms of radius (R) and wear scar angle (θ);

(ii) differentiate the expression to yield $\frac{dV_w}{d\theta}$;

(iii) determine the derivative of E_d with respect to θ, $\frac{dE_d}{d\theta}$, based on the assumption that the wear rate is inversely proportional to the wear scar width or on the assumptions that wear rate is inversely proportional to the wear scar area;

(iv) integrate $\frac{dE_d}{d\theta}$ to find an expression for E_d (and E_{dat}) in terms of θ;

(v) express V_w and E_{dat} as an infinite sum of polynomial terms (Taylor series) and approximate their expressions by taking their first non-constant polynomial terms;

(vi) express V_w as a function of E_{dat}.

A4.1 Cylinder-on-flat configuration assuming either wear scar width or wear scar area dependence of instantaneous wear rate

Find V_w. As shown in the previous study [8], finding V_w can be simplified as a geometric problem, i.e. V_w can be written as a function in terms of R and θ. For the cylinder-on-flat configuration, V_w can be approximated as the volume of a minor segment of a cylinder. Therefore, it can be shown that:

$$V_w = LR^2(\theta - \sin(\theta)\cos(\theta)) \qquad (A4.1.1)$$

where terms are as previously defined.

Calculate $\frac{dV_w}{d\theta}$. The derivative of V^w with respect to θ can be shown to be:

$$\frac{dV_w}{d\theta} = LR^2(1 - \cos(2\theta)) \qquad (A4.1.2)$$

Determine $\frac{dE_d}{d\theta}$. It was proposed in [8] that wear rate $\left(\frac{dV_w}{dE_d}\right)$ is dependent upon the scar width (x) in the following relationship:

$$\frac{dV_w}{dE_d} = \frac{k_1}{x} \qquad (A4.1.3)$$

For the cylinder-on-flat configuration, wear scar width is roughly uniform throughout the damaged area. Therefore, x can be approximated as the chord length of the minor segment, which is:

$$x = 2R\sin(\theta)$$

Therefore, the wear rate expression can be rewritten as:

$$\frac{dV_w}{d\theta}\frac{d\theta}{dE_d} = \frac{k_1}{2R\sin(\theta)} \qquad (A4.1.4)$$

Substituting Equation A4.1.2 into Equation A4.1.4 yields:

$$LR^2(1-\cos(2\theta))\frac{d\theta}{dE_d} = \frac{k_1}{2R\sin(\theta)}$$

which can be rearranged as follows:

$$\frac{dE_d}{d\theta} = \frac{2LR^3(1-\cos(2\theta))\sin(\theta)}{k_1} \qquad (A4.1.5)$$

Integrate $\frac{dE_d}{d\theta}$. E_d can be calculated by taking the integral of both sides of Equation A4.1.5 with respect to θ:

$$E_d = \frac{2LR^3}{k_1}\int (1-\cos(2\theta))\sin(\theta)\, d\theta$$

By use of trigonometric identities, this can be integrated as follows:

$$\int (1-\cos(2\theta))\sin(\theta)\ d\theta \equiv \frac{1}{2}\int 3\sin(\theta) - \sin(3\theta)\, d\theta = \frac{1}{2}\left(\frac{1}{3}\cos(3\theta) - 3\cos(\theta)\right) + c_1$$

where: c_1 is a constant of integration.

Substituting the integral of $(1-\cos(2\theta))\sin(\theta)$ into the expression for E_d gives:

$$E_d = \frac{LR^3}{3k_1}(\cos(3\theta) - 9\cos(\theta)) + \frac{2LR^3}{k_1}c_1$$

which can be rewritten as:

$$E_d = m_1 LR^3(\cos(3\theta) - 9\cos(\theta)) + C_1 \qquad (A4.1.6)$$

where: $m_1 = \frac{1}{3k_1}$;

$C_1 = \frac{2LR^3}{k_1}c_1$.

To evaluate the constant, C_1, it is noted that in a fretting contact, there is a threshold of energy dissipated, E_{th}, below which $\theta = 0$ (i.e. there is no wear); in this region, Equation A4.1.6 does not describe the relationship between E_d and θ. However, once E_d has exceeded E_{th}, then wear occurs (and thus $\theta > 0$). Evaluating Equation A4.1.6 when $E_d = E_{th}$ and $\theta = 0$ yields the following:

$$E_{th} = -8m_1 LR^3 + C_1$$

and thus:

$$C_1 = E_{th} + 8m_1LR^3$$

Substituting the expression of C_1 into Equation A4.1.6, the final equation for E_d is:

$$E_d = m_1LR^3(\cos(3\theta) - 9\cos(\theta) + 8) + E_{th} \qquad (A4.1.7)$$

A new term (E_{dat}) can be defined, which represents the frictional energy dissipated above the threshold energy for wear to commence so that $E_{dat} = E_d - E_{th}$ (the subscript "dat" being an acronym for "dissipated above threshold").

In summary, a parametric function of V_w and E_{dat} in terms of θ for the cylinder-on-flat configuration has been obtained:

$$\begin{pmatrix} V_w(\theta) \\ \\ E_{dat}(\theta) \end{pmatrix} = \begin{pmatrix} LR^2(\theta - \sin(\theta)\cos(\theta)) \\ \\ m_1LR^3(\cos(3\theta) - 9\cos(\theta) + 8) \end{pmatrix} \qquad (A4.1.8)$$

Express V_w and E_{dat} as an infinite polynomial sum (Taylor series). With the parametric function, V_w and E_d can both be represented as a Taylor series.

The definition of a Taylor series expansion of a function $f(x)$ at a point $x = a$ is as follows:

$$f(x) = \sum_{n=0}^{\infty} \frac{f^{(n)}(a)}{n!}(x-a)^n$$

where: $f^{(n)}(a) =$ the n^{th} derivative of $f(x)$ with respect to x evaluated at $x = a$.

Finding the Taylor series for V_w and E_{dat} at the point $\theta = 0$ (the Taylor series of a function at 0 is also known as a Maclaurin series), then V_w and E_{dat} can be written as:

$$\begin{pmatrix} V_w(\theta) \\ \\ E_{dat}(\theta) \end{pmatrix} = \begin{pmatrix} \sum_{n=0}^{\infty} \frac{V_w^{(n)}(0)}{n!}\theta^n \\ \\ \sum_{m=0}^{\infty} \frac{E_{dat}^{(m)}(0)}{k!}\theta^m \end{pmatrix}$$

Express V_w as a function of E_{dat}. The first-degree polynomial term of each Taylor series for both V_w and E_{dat} were taken as approximations as follows:

$$\begin{pmatrix} V_w(\theta) \\ \\ E_{dat}(\theta) \end{pmatrix} \approx \begin{pmatrix} \frac{2}{3}LR^2\theta^3 \\ \\ 3m_1LR^3\theta^4 \end{pmatrix} \qquad (A4.1.9)$$

Eliminating the parameter θ from the parametric equations in Equation A4.1.9 yields:

$$V_w = \frac{2}{3^{1.75}}\left(\frac{L}{m_1^3}\right)^{0.25} R^{-0.25} E_{dat}^{0.75} \qquad (A4.1.10)$$

A4.2 Sphere-on-flat configuration assuming wear scar width dependence of instantaneous wear rate

Find V_w. For the sphere-on-flat configuration, V_w can be approximated as the volume of a spherical cap, which is given by the following equation:

$$V_w = \frac{\pi R^3}{3}(\cos^3(\theta) - 3\cos(\theta) + 2) \qquad (A4.2.1)$$

where terms are as previously defined.

Calculate $\frac{dV_w}{d\theta}$. Using trigonometric identities, it can be shown that:

$$\cos^3(\theta) - 3\cos(\theta) + 2 \equiv \frac{\cos(3\theta) - 9\cos(\theta) + 8}{4}$$

Accordingly, the expression for V_w for the sphere-on-flat configuration (Equation A4.2.1) can be written as follows:

$$V_w = \frac{\pi R^3}{12}(\cos(3\theta) - 9\cos(\theta) + 8)$$

The derivative of V_w with respect to θ for the sphere-on-flat configuration can thus be written as follows:

$$\frac{dV_w}{d\theta} = \pi R^3 \sin^3(\theta) \qquad (A4.2.2)$$

Determine $\frac{dE_d}{d\theta}$. As has been shown for the cylinder-on-flat contact geometry, it is again proposed that wear rate ($\frac{dV_w}{dE_d}$) is dependent upon the width of the wear scar. In this case, the shape of the wear scar approximates to that of a circle, and therefore (in contrast to the cylinder-on-flat geometry), the wear scar width in the direction of fretting displacement is not uniform. As such, it is assumed that the instantaneous wear rate is inversely proportional to a characteristic wear scar width which is defined as the maximum width of the wear scar (i.e. the wear scar diameter, $2r$) as follows:

$$\frac{dV_w}{dE_d} = \frac{k_2}{2r} \qquad (A4.2.3)$$

Using the geometrical relationship:

$$r = R\sin(\theta)$$

the expression for the wear rate can be rewritten as follows:

$$\frac{dV_w}{d\theta}\frac{d\theta}{dE_d} = \frac{k_2}{2R\sin(\theta)} \qquad (A4.2.4)$$

Substituting Equation A4.2.2 into Equation A4.2.4 and rearranging yields:

$$\frac{dE_d}{d\theta} = \frac{2\pi R^4 \sin^4(\theta)}{k_2} \qquad (A4.2.5)$$

Integrate $\frac{dE_d}{d\theta}$. E_d can be calculated by taking the integral of Equation A4.2.5 with respect to θ:

$$E_d = \frac{2\pi R^4}{k_2}\int \sin^4(\theta)\ d\theta$$

By use of trigonometric identities, this can be integrated as follows:

$$\int \sin^4(\theta)\, d\theta \equiv \frac{1}{8}\int \cos(4\theta) - 4\cos(2\theta) + 3\, d\theta\ = \frac{1}{32}(\sin(4\theta) - 8\sin(2\theta) + 12\theta) + c_2$$

where: c_2 is a constant of integration.

Substituting the integral of $\sin^4(\theta)$ into the expression for E_d yields:

$$E_d = \frac{\pi R^4}{16k_2}(\sin(4\theta) - 8\sin(2\theta) + 12\theta) + \frac{2\pi R^4}{k_2}c_2$$

which can be rewritten as:

$$E_d = m_2\pi R^4(\sin(4\theta) - 8\sin(2\theta) + 12\theta) + C_2 \qquad (A4.2.6)$$

where: $m_2 = \frac{1}{16k_2}$;

$C_2 = \frac{2\pi R^4}{k_2}c_2$.

As previously, it can be seen that the constant C_2 can be evaluated as follows:

$$C_2 = E_{th}$$

A final equation for E_{dat} can therefore be written as follows:

$$E_{dat} = m_2\pi R^4(\sin(4\theta) - 8\sin(2\theta) + 12\theta) \qquad (A4.2.7)$$

In summary, a parametric function of V_w and E_{dat} in terms of θ for the sphere-on-flat configuration assuming wear scar width dependence of instantaneous wear rate has been obtained:

$$\begin{pmatrix} V_w(\theta) \\ \\ E_{dat}(\theta) \end{pmatrix} = \begin{pmatrix} \frac{\pi R^3}{12}(\cos(3\theta) - 9\cos(\theta) + 8) \\ \\ m_2\pi R^4(\sin(4\theta) - 8\sin(2\theta) + 12\theta) \end{pmatrix} \qquad (A4.2.8)$$

Express V_w and E_{dat} as an infinite polynomial sum (Taylor series). With the establishment of the parametric function, the Taylor series for V_w and E_d can be expressed as follows:

$$\begin{pmatrix} V_w(\theta) \\ E_{dat}(\theta) \end{pmatrix} = \begin{pmatrix} \sum_{n=0}^{\infty} \frac{V_w^{(n)}(0)}{n!}\theta^n \\ \sum_{m=0}^{\infty} \frac{E_{dat}^{(m)}(0)}{k!}\theta^m \end{pmatrix}$$

Express V_w as a function of E_d. The first non-constant term of each Taylor series for both V_w and E_{dat} were taken as approximations as follows:

$$\begin{pmatrix} V_w(\theta) \\ E_{dat}(\theta) \end{pmatrix} \approx \begin{pmatrix} \frac{\pi R^3 \theta^4}{4} \\ \frac{32}{5} m_2 \pi R^4 \theta^5 \end{pmatrix} \quad (A4.2.9)$$

Eliminating the parameter θ from the parametric equations in Equation A4.2.9 yields:

$$V_w = \frac{1}{4}\left(\frac{5}{32}\right)^{0.8}\left(\frac{\pi}{m_2^4}\right)^{0.2} R^{-0.2} E_{dat}^{0.8} \quad (A4.2.10)$$

A4.3 Sphere-on-flat configuration assuming wear scar area dependence of instantaneous wear rate

Find V_w. The expression of V_w as a function of R and θ remains the same as Equation A4.2.1:

$$V_w = \frac{\pi R^3}{3}(\cos^3(\theta) - 3\cos(\theta) + 2) \quad (A4.3.1)$$

where terms are as previously defined.

Calculate $\frac{dV_w}{d\theta}$. Direct use of Equation A4.2.2:

$$\frac{dV_w}{d\theta} = \pi R^3 \sin^3(\theta) \quad (A4.3.2)$$

Determine $\frac{dE_d}{d\theta}$. The assumption here is that the wear rate ($\frac{dV_w}{dE_d}$) is dependent upon the area of the wear scar (A). In this case, the shape of the wear scar approximates to that of a circle, and therefore (in contrast to the cylinder-on-flat geometry), the maximum width of the wear scar ($2R\sin(\theta)$) is defined as the diameter of the wear scar area $2r$:

$$\frac{dV_w}{dE_d} = \frac{k_2'}{A} \quad (A4.3.3)$$

Using the geometrical relationship:

$$A = \pi r^2 = \pi R^2 \sin^2(\theta)$$

the expression for the wear rate can be rewritten as follows:

$$\frac{dV_w}{d\theta}\frac{d\theta}{dE_d} = \frac{k_2'}{\pi R^2 \sin^2(\theta)} \qquad (A4.3.4)$$

Substituting Equation A4.3.2 into Equation A4.3.4 and rearranging yields:

$$\frac{dE_d}{d\theta} = \frac{\pi^2 R^5 \sin^5(\theta)}{k_2'} \qquad (A4.3.5)$$

Integrate $\frac{dE_d}{d\theta}$. E_d can be calculated by taking the integral of Equation A4.3.5 with respect to θ:

$$E_d = \frac{\pi^2 R^5}{k_2'}\int \sin^5(\theta)\ d\theta$$

By use of trigonometric identities, this can be integrated as follows:

$$\int \sin^5(\theta)\, d\theta \equiv \frac{1}{16}\int \sin(5\theta) - 5\sin(3\theta) + 10\sin(\theta)\, d\theta$$
$$= \frac{1}{240}(-3\cos(5\theta) + 25\cos(3\theta) - 150\cos(\theta)) + c_2'$$

where: $c_2'$is a constant of integration.

Substituting the integral of $\sin^5(\theta)$ into the expression for E_d yields:

$$E_d = \frac{\pi^2 R^5}{240k_2'}(-3\cos(5\theta) + 25\cos(3\theta) - 150\cos(\theta)) + \frac{\pi^2 R^4}{k_2'}c_2'$$

which can be rewritten as:

$$E_d = m_2'\pi^2 R^5(-3\cos(5\theta) + 25\cos(3\theta) - 150\cos(\theta)) + C_2' \qquad (A4.3.6)$$

where: $m_2' = \frac{1}{240k_2'}$;

$C_2' = \frac{\pi^2 R^5}{k_2'}c_2'$.

As previously, it can be seen that the constant C_2' can be evaluated as follows:

$$C_2' = E_{th} + 128m_2'\pi^2 R^5$$

A final equation for E_{dat} can therefore be written as follows:

$$E_{dat} = m_2'\pi^2 R^5(-3\cos(5\theta) + 25\cos(3\theta) - 150\cos(\theta) + 128) \qquad (A4.3.7)$$

In summary, a parametric function of V_w and E_{dat} in terms of θ for the sphere-on-flat configuration assuming wear scar area dependence of instantaneous wear rate has been obtained:

$$\begin{pmatrix} V_w(\theta) \\ \\ E_{dat}(\theta) \end{pmatrix} = \begin{pmatrix} \frac{\pi R^3}{12}(\cos(3\theta) - 9\cos(\theta) + 8) \\ \\ m_2'\pi^2 R^5(-3\cos(5\theta) + 25\cos(3\theta) - 150\cos(\theta) + 128) \end{pmatrix} \qquad (A4.3.8)$$

Express V_w and E_{dat} as an infinite polynomial sum (Taylor series). With the establishment of the parametric function, the Taylor series for V_w and E_d can be expressed as follows:

$$\begin{pmatrix} V_w(\theta) \\ \\ E_{dat}(\theta) \end{pmatrix} = \begin{pmatrix} \sum_{n=0}^{\infty} \frac{V_w^{(n)}(0)}{n!}\theta^n \\ \\ \sum_{m=0}^{\infty} \frac{E_{dat}^{(m)}(0)}{k!}\theta^m \end{pmatrix}$$

Express V_w as a function of E_d. The first non-constant term of each Taylor series for both V_w and E_{dat} were taken as approximations as follows:

$$\begin{pmatrix} V_w(\theta) \\ \\ E_{dat}(\theta) \end{pmatrix} \approx \begin{pmatrix} \frac{\pi R^3 \theta^4}{4} \\ \\ 40 m_2'\pi^2 R^5 \theta^6 \end{pmatrix} \qquad (A4.3.9)$$

Eliminating the parameter θ from the parametric equations in Equation A4.3.9 yields:

$$V_w = \frac{1}{4}\left(\frac{1}{40}\right)^{0.67}\left(\frac{1}{\pi m_2'^{\,2}}\right)^{0.33} R^{-0.33} E_{dat}^{0.67} \qquad (A4.3.10)$$

A4.4 Crossed-cylinder configuration assuming wear scar width dependence of instantaneous wear rate

Find V_w. For the crossed-cylinder configuration, defining the shape of the intersection between two orthogonally crossed cylinders is not straightforward, and therefore the derivation of V^w is similarly not straightforward.

We define the system as two orthogonally crossed cylinders with the same radius (R) in cartesian coordinates. The shortest distance between the central axes of these two cylinders, $2d$, is defined as follows:

$$2d = R + R\cos(\theta)$$

The axis of one cylinder $(cylinder\ a)$ has its axis parallel to the x-axis and crosses the z-axis at $z = d$, whilst the axis of the other cylinder $(cylinder\ b)$ is parallel to the y-axis and crosses the z-axis at $z = -d$. This geometry is illustrated in Figure 17.

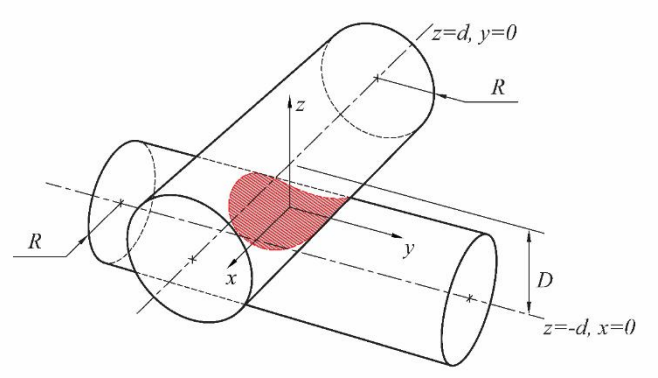

Figure 17: Illustration of two orthogonally crossed cylinders with identical radius (R) in cartesian coordinates. The distance between their central axes is D.

For $cylinder\ a$, all the points inside satisfy the inequality that:

$$y^2 + (z-d)^2 \leq R^2$$

For $cylinder\ b$, all the points inside satisfy the inequality that:

$$x^2 + (z+d)^2 \leq R^2$$

Rearranging these two inequalities gives the boundary of the intersection on x-axis and y-axis:

$$|y| \leq \sqrt{R^2 - (z-d)^2}$$

$$|x| \leq \sqrt{R^2 - (z+d)^2}$$

The limits on the z-axis are determined by the requirement that the arguments of both the square roots in the above inequalities are not negative:

$$-R \leq z - d$$
$$z + d \leq R$$

Therefore:

$$d - R \leq z \leq R - d$$

As shown in Figure 18, every cross-section parallel to the $x-y$ plane is a rectangle with sides of length l_1 and l_2. Therefore, the volume of the intersection can be described as:

$$V_w = \lim_{n\to\infty} \sum_{j=1}^{n} l_1(z_j) l_2(z_j) \Delta z$$

where:

$$\Delta z = \frac{2R - 2d}{n}$$

$$z_j = (d - R) + \Delta z \cdot j$$

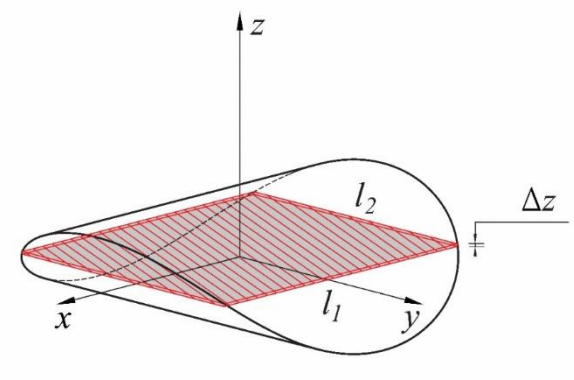

Figure 18: Illustration of the intersection volume being calculated by integration of each slice parallel to the $x - y$ plane within the boundary.

As $n \to +\infty$, the volume of the intersection can be written as an integral:

$$V_w = \int_{d-R}^{R-d} l_1(z) l_2(z)\, dz$$

Since l_1 is a line segment defined by the boundary of the intersection on x-axis, and l_2 is defined by the boundary on y-axis, the following equations can be derived:

$$l_1 = 2\sqrt{R^2 - (z+d)^2}$$
$$l_2 = 2\sqrt{R^2 - (z-d)^2}$$

Therefore, V_w can be expressed as:

$$V_w = \int_{d-R}^{R-d} 4\sqrt{(R^2 - (z+d)^2)(R^2 - (z-d)^2)}\, dz = 8\int_0^{R-d} \sqrt{(R^2 - (z+d)^2)(R^2 - (z-d)^2)}\, dz$$

Rearranging this equation yields:

$$V_w = 8\int_0^{R-d} \sqrt{((R-d)^2 - z^2)((R+d)^2 - z^2)}\, dz$$

Let:

$$z = (R-d)\sin(\theta)$$

Then:

$$dz = (R-d)\cos(\theta)\, d\theta$$

Changing the variable of the integration gives:

$$V_w = 8\int_0^{\frac{\pi}{2}} \sqrt{(R-d)^2\cos^2(\theta)}\sqrt{(R+d)^2 - (R-d)^2\sin^2(\theta)}\ (R-d)\cos(\theta)\, d\theta$$

Rearranging this equation yields:

$$V_w = 8(R-d)^2(R+d)\int_0^{\frac{\pi}{2}} \cos^2(\theta)\sqrt{1-\left(\frac{R-d}{R+d}\right)^2 \sin^2(\theta)}\ d\theta$$

To solve this integral, a standard formula [26] (Chapter 3.67 - "Square roots of expressions containing trigonometric functions") is applied:

$$\int_0^{\frac{\pi}{2}} \sin^{\alpha}(x)\cos^{\beta}(x)\sqrt{1-k^2\sin^2(x)}\ dx = \frac{1}{2}\mathrm{B}\left(\frac{\alpha+1}{2},\frac{\beta+1}{2}\right)\mathrm{F}\left(\frac{\alpha+1}{2},-\frac{1}{2};\frac{\alpha+\beta+2}{2};k^2\right)$$

for

$$\alpha > -1;\ \beta > -1;\ |k| < 1$$

In the expression of V_w, it can be found that:

$$\alpha = 0;\ \beta = 2;\ k = \frac{R-d}{R+d}$$

Therefore, an expression for V_w can be written as follows:

$$V_w = 8(R-d)^2(R+d)\cdot\frac{1}{2}\mathrm{B}\left(\frac{1}{2},\frac{3}{2}\right)\mathrm{F}\left(\frac{1}{2},-\frac{1}{2};2;\left(\frac{R-d}{R+d}\right)^2\right) \qquad (A4.4.1)$$

This can be solved to yield:

$$V_w = \frac{\pi R^3}{4}(\cos^3(\theta)+\cos^2(\theta)-5\cos(\theta)+3) \qquad (A4.4.2)$$

where terms are previously defined. For the detailed derivation of Equation A4.4.2 from Equation A4.4.1, see Section A4.5.

Using trigonometric identities, it can be shown that:

$$\cos^3(\theta)+\cos^2(\theta)-5\cos(\theta)+3 \equiv \frac{1}{4}(\cos(3\theta)+2\cos(2\theta)-17\cos(\theta)+14)$$

which leads to:

$$V_w = \frac{\pi R^3}{16}(\cos(3\theta)+2\cos(2\theta)-17\cos(\theta)+14) \qquad (A4.4.3)$$

Calculate $\frac{dV_w}{d\theta}$. The derivative of V_w with respect to θ can be shown to be:

$$\frac{dV_w}{d\theta} = \frac{\pi R^3}{4}\sin(\theta)(-3\cos^2(\theta)-2\cos(\theta)+5) \qquad (A4.4.4)$$

Determine $\frac{dE_d}{d\theta}$. It is proposed that wear rate ($\frac{dV_w}{dE_d}$) is also dependent upon the scar width (x) for the crossed-cylinder configuration:

$$\frac{dV_w}{dE_d} = \frac{k_3}{x}$$

However, the wear scar width in the direction of fretting movement is not uniform across the damaged area for the crossed-cylinders configuration. A characteristic wear scar width is defined as the maximum width of the wear scar, which is given by the following:

$$x = 2R\sin(\theta)$$

Therefore, the wear rate expression can be rewritten as:

$$\frac{dV_w}{d\theta}\frac{d\theta}{dE_d} = \frac{k_3}{2R\sin(\theta)} \qquad (A4.4.5)$$

Substituting Equation A4.4.4 into Equation A4.4.5 gives:

$$\frac{\pi R^3}{4}\sin(\theta)(-3\cos^2(\theta) - 2\cos(\theta) + 5)\frac{d\theta}{dE_d} = \frac{k_3}{2R\sin(\theta)}$$

which can be rearranged to yield:

$$\frac{dE_d}{d\theta} = \frac{\pi R^4 \sin^2(\theta)\,(-3\cos^2(\theta) - 2\cos(\theta) + 5)}{2k_3} \qquad (A4.4.6)$$

Integrate $\frac{dE_d}{d\theta}$. E_d can be calculated by taking the integral of Equation A4.4.6 with respect to θ:

$$E_d = \frac{\pi R^4}{2k_3}\int \sin^2(\theta)\,(-3\cos^2(\theta) - 2\cos(\theta) + 5)\,d\theta$$

By use of well-known trigonometric identities, this can be integrated as follows:

$$\begin{aligned}
&\int \sin^2(\theta)\,(-3\cos^2(\theta) - 2\cos(\theta) + 5)\,d\theta \\
&\equiv \frac{1}{8}\int 3\cos(4\theta) + 4\cos(3\theta) - 20\cos(2\theta) - 4\cos(\theta) + 17\,d\theta \\
&= \frac{1}{96}(9\sin(4\theta) + 16\sin(3\theta) - 120\sin(2\theta) - 48\sin(\theta) + 204\theta) + c_3
\end{aligned}$$

where: c_3 is a constant of integration.

Substituting the integral of $\sin^2(\theta)\,(-3\cos^2(\theta) - 2\cos(\theta) + 5)$ into the expression for E_d yields:

$$E_d = \frac{\pi R^4}{192k_3}(9\sin(4\theta) + 16\sin(3\theta) - 120\sin(2\theta) - 48\sin(\theta) + 204\theta) + \frac{\pi R^4}{192k_3}c_3$$

which can be rewritten as:

$$E_d = m_3\pi R^4(9\sin(4\theta) + 16\sin(3\theta) - 120\sin(2\theta) - 48\sin(\theta) + 204\theta) + C_3 \qquad (A4.4.7)$$

where:

$$m_3 = \frac{1}{192k_3}$$

and

$$C_3 = \frac{\pi R^4}{192k_3}c_2$$

As previously, it can be seen that the constant C_3 can be evaluated as follows:

$$C_3 = E_{th}$$

A final equation for E_{dat} can therefore be written as follows:

$$E_{dat} = m_3\pi R^4(9\sin(4\theta) + 16\sin(3\theta) - 120\sin(2\theta) - 48\sin(\theta) + 204\theta) \qquad (A4.4.8)$$

Therefore, a set of parametric function of V^w and E_d in terms of θ for the crossed-cylinders configuration has been obtained:

$$\begin{pmatrix} V_w(\theta) \\ E_{dat}(\theta) \end{pmatrix} = \begin{pmatrix} \frac{\pi R^3}{16}(\cos(3\theta) + 2\cos(2\theta) - 17\cos(\theta) + 14) \\ m_3\pi R^4(9\sin(4\theta) + 16\sin(3\theta) - 120\sin(2\theta) - 48\sin(\theta) + 204\theta) \end{pmatrix} \qquad (A4.4.9)$$

Expand V_w and E_{dat} as an infinite polynomial sum (Taylor series). With the establishment of the parametric function, the Taylor series for V_w and E_d can be expressed as follows:

$$\begin{pmatrix} V_w(\theta) \\ E_{dat}(\theta) \end{pmatrix} = \begin{pmatrix} \sum_{n=0}^{\infty} \frac{V_w^{(n)}(0)}{n!}\theta^n \\ \sum_{m=0}^{\infty} \frac{E_{dat}^{(m)}(0)}{k!}\theta^m \end{pmatrix}$$

Express V^w as a function of E_d. The first non-constant term of each Taylor series for both V_w and E_{dat} were taken as approximations as follows:

$$\begin{pmatrix} V_w(\theta) \\ E_{dat}(\theta) \end{pmatrix} \approx \begin{pmatrix} \frac{\pi R^3\theta^4}{4} \\ \frac{384}{5}m_3\pi R^4\theta^5 \end{pmatrix} \qquad (A4.4.10)$$

Eliminating the parameter θ from the parametric equations in Equation A4.4.10 yields:

$$V_w = \frac{1}{4}\left(\frac{5}{384}\right)^{0.8}\left(\frac{\pi}{m_3^4}\right)^{0.2} R^{-0.2}E_{dat}^{0.8} \qquad (A4.4.11)$$

A4.5 The beta function, gamma function and hypergeometric function

In the previous section (Section A4.4), an expression for V_w for a crossed-cylinders contact was written in the form of Equation A4.4.1. The right side of the equation involves the use of the Beta function, B, the Gamma function, Γ, and the Hypergeometric function, F.

The definition of the Beta function is given by:

$$\mathrm{B}(x,y) = \int_0^1 t^{x-1}(1-t)^{y-1}\,dt\,, \qquad \mathrm{Re}(x) > 0; \mathrm{Re}(y) > 0$$

The Gamma function is an extension of the factorial function from positive integers to complex numbers, and its definition is:

$$\Gamma(z) = \int_0^\infty t^{z-1}e^{-t}\,dt\,, \qquad \mathrm{Re}(z) > 0$$

There is an important relationship between Beta function and Gamma function (for a proof, see Chapter 2 of Artin's book “The Gamma Function” [27]):

$$\mathrm{B}(x,y) = \frac{\Gamma(x)\Gamma(y)}{\Gamma(x+y)}$$

As such, the Beta function in Equation A4.4.1 is equal to:

$$\mathrm{B}\left(\frac{1}{2},\frac{3}{2}\right) = \frac{\Gamma\left(\frac{1}{2}\right)\Gamma\left(\frac{3}{2}\right)}{\Gamma(2)} \qquad (A4.5.1)$$

With the definition of Γ, it can be shown that:

$$\Gamma(z+1) = \int_0^\infty t^z e^{-t}\,dt$$

Let:

$$\frac{du}{dt} = e^{-t}$$
$$v = t^z$$

which yields:

$$u = -e^{-t}$$
$$\frac{dv}{dt} = zt^{z-1}$$

Thus:

$$\Gamma(z+1) = -t^z e^{-t}\Big|_0^\infty + \int_0^\infty z t^{z-1} e^{-t}\, dt = \lim_{t\to\infty}(-t^z e^{-t}) - (0e^0) + \int_0^\infty z t^{z-1} e^{-t}\, dt$$

As $t \to +\infty$, $-t^z e^{-t} \to 0$, which means that $\Gamma(z+1)$ can be written as:

$$\begin{aligned}\Gamma(z+1) &= z\int_0^\infty t^{z-1} e^{-t}\, dt \\ &= z\Gamma(z)\end{aligned}$$

Equation A4.5.1 can therefore be simplified as follows:

$$\begin{aligned}\mathrm{B}\left(\frac{1}{2},\frac{3}{2}\right) &= \frac{\Gamma\left(\frac{1}{2}\right)\Gamma\left(\frac{1}{2}+1\right)}{\Gamma(1+1)} \\ &= \frac{1}{2}\frac{\Gamma\left(\frac{1}{2}\right)^2}{\Gamma(1)}\end{aligned} \qquad (A4.5.2)$$

The gamma functions $\Gamma\left(\frac{1}{2}\right)$ and $\Gamma(1)$ can be evaluated as follows:

$$\Gamma\left(\frac{1}{2}\right) = \int_0^\infty t^{-\frac{1}{2}} e^{-t}\, dt$$

$$\Gamma(1) = \int_0^\infty e^{-t}\, dt$$

For $\Gamma\left(\frac{1}{2}\right)$, let:

$$t = u^2$$

then:

$$dt = 2u\, du$$

which leads to:

$$\Gamma\left(\frac{1}{2}\right) = 2\int_0^\infty e^{-u^2}\, du$$

Recognizing that the right-hand side of the equation for $\Gamma\left(\frac{1}{2}\right)$ is the Gaussian integral, which is evaluated as follows:

$$\int_{-\infty}^\infty e^{-x^2}\, dx = \sqrt{\pi}$$

therefore:

$$\Gamma\left(\frac{1}{2}\right) = \sqrt{\pi} \qquad (A4.5.3)$$

The value of $\Gamma(1)$ can be readily evaluated as:

$$\begin{aligned}\Gamma(1) &= \int_0^{\infty} e^{-t}\,dt \\ &= \lim_{t\to\infty}(-e^{-t}) - (-e^{0}) \\ &= 1\end{aligned} \qquad (A4.5.4)$$

Substituting Equation A4.5.3 and Equation A4.5.4 into the Beta function in Equation A4.5.1 yields:

$$\begin{aligned}\mathrm{B}\left(\frac{1}{2},\frac{3}{2}\right) &= \frac{1}{2}\frac{\Gamma\left(\frac{1}{2}\right)^2}{\Gamma(1)} \\ &= \frac{1}{2}\frac{\left(\sqrt{\pi}\right)^2}{1} \\ &= \frac{\pi}{2}\end{aligned} \qquad (A4.5.5)$$

In addition to Beta function and gamma function, Equation A4.4.1 requires the knowledge of Hypergeometric function, F, which is defined by the Gaussian series:

$$\begin{aligned}\mathrm{F}(a,b;c;z) &= \sum_{n=0}^{\infty}\frac{(a)_n(b)_n}{(c)_n}\frac{z^n}{n!} \\ &= 1 + \frac{ab}{c}z + \frac{a(a+1)b(b+1)}{c(c+1)}\frac{z^2}{2!} + \cdots\end{aligned}$$

Therefore, by substituting the values $a = \frac{1}{2}$, $b = \frac{3}{2}$, $c = 2$ and $z = \left(\frac{R-d}{R+d}\right)^2$, the Hypergeometric function in Equation A4.4.1 can be written as follows:

$$\mathrm{F}\left(\frac{1}{2},-\frac{1}{2};2;\left(\frac{R-d}{R+d}\right)^2\right) = 1 - \frac{1}{8}\left(\frac{R-d}{R+d}\right)^2 - \frac{1}{64}\left(\frac{R-d}{R+d}\right)^4 + \cdots \qquad (A4.5.6)$$

It is noted that from the second term of the Gaussian series for $\mathrm{F}\left(\frac{1}{2},-\frac{1}{2};2;\left(\frac{R-d}{R+d}\right)^2\right)$, the absolute coefficient has dropped to $\frac{1}{8}$ or even less, meaning it is reasonable to take only the first term as the approximation of the whole series. Therefore, we can simplify the Hypergeometric function in Equation A4.4.1 as follows:

$$\mathrm{F}\left(\frac{1}{2},-\frac{1}{2};2;\left(\frac{R-d}{R+d}\right)^2\right) \approx 1 \qquad (A4.5.7)$$

With the knowledge of the Beta function, $\mathrm{B}\left(\frac{1}{2},\frac{3}{2}\right)$, and the Hypergeometric function, $\mathrm{F}\left(\frac{1}{2},-\frac{1}{2};2;\left(\frac{R-d}{R+d}\right)^2\right)$, Equation A4.4.1 can be evaluated as follows:

$$V_w = 8(R-d)^2(R+d)\cdot\frac{1}{2}\mathrm{B}\left(\frac{1}{2},\frac{3}{2}\right)\mathrm{F}\left(\frac{1}{2},-\frac{1}{2};2;\left(\frac{R-d}{R+d}\right)^2\right)$$
$$\approx 8(R-d)^2(R+d)\cdot\frac{1}{2}\frac{\pi}{2}\cdot 1$$
$$\approx 2\pi(R-d)^2(R+d) \qquad (A4.5.8)$$

Since:

$$d = \frac{R + R\cos(\theta)}{2}$$

the expression for V_w in Equation A4.5.8 can be written as:

$$V_w \approx 2\pi(R^2-d^2)(R-d)$$
$$\approx 2\pi R^3\left(\frac{3-2\cos(\theta)-\cos^2(\theta)}{4}\right)\left(\frac{1-\cos(\theta)}{2}\right)$$

Finally, rearranging the equation above gives:

$$V_w \approx \frac{\pi R^3}{4}(\cos^3(\theta)+\cos^2(\theta)-5\cos(\theta)+3) \qquad (A4.5.9)$$

To understand the error associated with this approximation, 3D modelling software was used to construct the shape of the intersection between two orthogonally crossed cylinders with varying θ. Using the software, the volume of intersection was evaluated numerically, and this was then compared with the approximated values evaluated by Equation A4.5.9. As can be seen from Figure 19, the differences between the normalised wear volume, v_w (where $v_w = \frac{4V_w}{\pi R^3}$), calculated by these two methods are negligible across the whole range of θ. It is therefore reasonable to assert that Equation A4.5.9 derived from the simplification of Equation A4.5.7 well describes the relationship between V_w and θ for the crossed-cylinder contact.

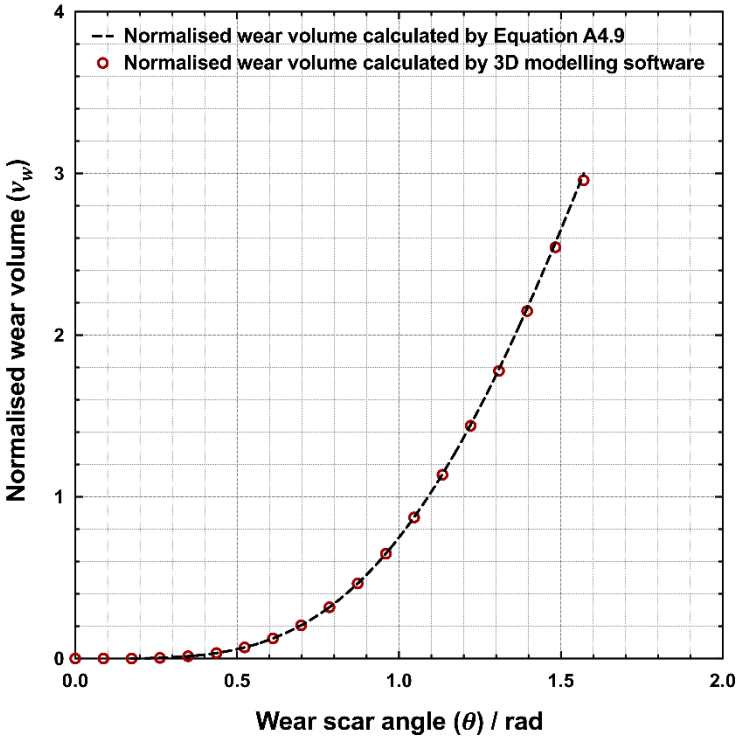

Figure 19: Plot of normalised wear volume evaluated numerically via 3D modelling software compared with equivalent values calculated from Equation A4.5.9.